Synthesis, Characterization, and Coordination Chemistry of a Novel Edge-Shared M_2L_9 Species, $Mo_2(\mu\text{-}S)(\mu\text{-}Cl)Cl_3(PMe_3)_4$

Keith A. Hall[1] and James M. Mayer*

Department of Chemistry, BG-10, University of Washington, Seattle, Washington 98195

Received October 7, 1994[⊗]

The d^3−d^3 M_2L_{10} dimer $Mo_2(\mu\text{-}S)(\mu\text{-}Cl)Cl_3(PMe_3)_5$ (**1**) readily and reversibly loses a phosphine ligand to produce the M_2L_9 species $Mo_2(\mu\text{-}S)(\mu\text{-}Cl)Cl_3(PMe_3)_4$ (**2**). An X-ray crystal structure of **2** reveals an unprecedented edge-shared structure, as opposed to the face-shared structure typical of M_2L_9 dimers. The phosphine ligand lost from **1** is the one *trans* to the μ-sulfido ligand, which has an exceptionally long Mo−P bond distance in **1**. Otherwise, the structure of **2** is similar to that of **1**, suggesting an analogous Mo(III)−Mo(III) assignment, with an Mo−Mo bond of 2.6293(8) Å and short Mo−S distances of 2.288(2) and 2.222(2) Å. The analogous M_2L_9 complexes $Mo_2(\mu\text{-}O)(\mu\text{-}Cl)Cl_3(PMe_3)_4$ and $W_2(\mu\text{-}S)(\mu\text{-}Cl)Cl_3(PMe_3)_4$ have also been observed. $Mo_2(\mu\text{-}S)(\mu\text{-}Cl)Cl_3(PMe_3)_4$ (**2**) reacts with chloride ion, acetonitrile, and carbon monoxide to give new M_2L_{10} dimer adducts, $[Mo_2(\mu\text{-}S)(\mu\text{-}Cl)Cl_4(PMe_3)_4]NMe_4$ (**5**[NMe_4]), $Mo_2(\mu\text{-}S)(\mu\text{-}Cl)Cl_3(PMe_3)_4(CH_3CN)$ (**6**), and $Mo_2(\mu\text{-}S)(\mu\text{-}Cl)Cl_3(PMe_3)_4(CO)$ (**7**, **8a**), the first two of which have been characterized by X-ray crystallography. The $Mo_2(\mu\text{-}S)(\mu\text{-}Cl)$ core is maintained in each of these dimers, with very similar metrical data, but adduct formation is accompanied by rearrangement of the other ligands. Alkynes react with **2** to form M_2L_{10} dimers with bridging sulfido and alkyne ligands, such as $Mo_2(\mu\text{-}S)(\mu\text{-}MeC{\equiv}CMe)Cl_4(PMe_3)_4$ (**10a**). The CO and 2-butyne adducts have labile phosphine ligands *trans* to the bridging sulfur atom, and M_2L_9 species analogous to **2** can be isolated. The structures, diamagnetism, and lability of phosphine ligands *trans* to the μ-sulfido (or -oxo) in these dimers are suggested to arise from strong S→M π-bonding in the $Mo_2(\mu\text{-}S)(\mu\text{-}X)$ core. Crystal data: for **2**·C_7H_8, *C*2/*c*, $Z = 8$, $a = 37.822(5)$ Å, $b = 9.6820(9)$ Å, $c = 22.249(3)$ Å, $V = 6635(3)$ Å^3, refined to $R = 4.3\%$, $R_w = 4.4\%$, GOF = 1.324; for **5**[NMe_4], $P2_1/n$, $Z = 4$, $a = 11.807(1)$ Å, $b = 16.105(2)$ Å, $c = 17.567(3)$ Å, $V = 3302.8(7)$ Å^3, refined to $R = 3.8\%$, $R_w = 5.4\%$, GOF = 1.10; for **6**, $P\bar{1}$, $Z = 2$, $a = 8.578(1)$ Å, $b = 10.176(1)$ Å, $c = 17.562(2)$ Å, $V = 1420.7(7)$ Å^3, refined to $R = 3.6\%$, $R_w = 4.3\%$, GOF = 1.114; for **10a**, *Pnma*, $Z = 4$, $a = 22.166(2)$ Å, $b = 13.979(1)$ Å, $c = 9.455(1)$ Å, $V = 2929.8(4)$ Å^3, refined to $R = 2.7\%$, $R_w = 3.8\%$, GOF = 0.71.

Transition metal dimer complexes have been a focus of inorganic chemistry for many years because of their potential for chemistry quite different from that of mononuclear species. The diverse coordination chemistry observed in metal dimers results from the presence of a variety of coordination sites, including bridging sites and terminal positions both *cis* and *trans* to the metal−metal vector. Much emphasis has been placed on the nature of the metal−metal interaction, how the metal−metal bond is affected by ancillary ligands and how it affects structural preferences, and the metal−metal bond as a site of reactivity.[2,3] Often metal−metal bonds possess significant π and δ bonding components giving rise to metal−metal multiple bonding,[2] analogous to metal−ligand multiple bonding, for instance in monomeric metal−sulfido complexes.[4] Surprisingly, however, there are few reports on the effect of strong π-donation from a ligand to a metal center in dimers where significant metal−metal interactions exist.[5] Such metal−ligand π-bonding can have interesting consequences for the structures and reactivities of metal dimers.

We recently reported the synthesis of an unusual M_2L_{10} dimer $Mo_2(\mu\text{-}S)(\mu\text{-}Cl)Cl_3(PMe_3)_5$ (**1**) from the reactions of $MoCl_2(PMe_3)_4$ with sulfur atom donors (eq 1) or by conproportionation

$$2\,MoCl_2(PMe_3)_4 + SPMe_3 \xrightarrow[C_6H_6]{80\,^\circ C} \mathbf{1} + 4\,PMe_3 \qquad (1)$$

of the molybdenum(IV) sulfido complex $Mo(S)Cl_2(PMe_3)_3$ with $MoCl_2(PMe_3)_4$. The analogous tungsten complex, $W_2(\mu\text{-}S)(\mu\text{-}Cl)Cl_3(PMe_3)_5$, and the molybdenum μ-oxo dimer $Mo_2(\mu\text{-}O)(\mu\text{-}Cl)Cl_3(PMe_3)_5$ can also be formed by conproportionation.[6]

Complex **1** adopts an edge-shared bioctahedral (ESBO) structure typical of dimers with ten ligands (M_2L_{10} species).[2] The presence of two different bridging ligands and odd numbers of terminal ligands leads to a low-symmetry (C_s) structure with four different phosphine ligand environments. The observation of short Mo−S bonds and a significant *trans* influence on the phosphine and chloride ligands opposite the sulfur, as well as a significant *trans*-labilizing effect on the phosphine ligands in

⊗ Abstract published in *Advance ACS Abstracts*, February 1, 1995.

(1) University of Washington David M. Ritter Fellow. Current address: Los Alamos National Laboratory, CST-18, Mail Stop J514, Los Alamos, NM 87545.

(2) (a) Cotton, F. A.; Walton, R. A. *Multiple Bonds Between Metal Atoms*, 2nd ed.; Oxford University Press: New York, 1993. (b) Cotton, F. A. *Polyhedron* **1987**, *6*, 667−677. (c) Messerle, L. *Chem. Rev.* **1988**, *88*, 1229−1254.

(3) *Reactivity of Metal−Metal Bonds*, Chisholm, M. H., Ed.; ACS Symposium Series; American Chemical Society: Washington, DC, 1981.

(4) (a) Müller, A.; Diemann, E. *Comprehensive Coordination Chemistry*; Wilkinson, G., Ed.; Pergamon Press: London, 1987; Vol. 2; pp 515−550. (b) Nugent, W. A.; Mayer, J. M. *Metal−Ligand Multiple Bonds*; Wiley-Interscience: New York, 1988.

(5) Bryan, J. C.; Wheeler, D. R.; Clark, D. L.; Huffman, J. C.; Sattelberger, A. P. *J. Am. Chem. Soc.* **1991**, *113*, 3184 and references therein.

(6) Hall, K. A.; Mayer, J. M. *Inorg. Chem.* **1994**, *33*, 3289−3298.

0020-1669/95/1334-1145$09.00/0

Table 1. Selected Bond Distances (Å) for $Mo_2(\mu\text{-}S)(\mu\text{-}Cl)Cl_3(PMe_3)_4 \cdot C_7H_8$ (**2**·C_7H_8)

Mo(1)−Mo(2)	2.6293(8)	Mo(2)−Cl(1)	2.438(2)
Mo(1)−Cl(1)	2.492(2)	Mo(2)−Cl(3)	2.343(2)
Mo(1)−Cl(2)	2.479(2)	Mo(2)−Cl(4)	2.344(2)
Mo(1)−S(1)	2.288(2)	Mo(2)−S(1)	2.222(2)
Mo(1)−P(1)	2.509(2)	Mo(2)−P(4)	2.494(2)
Mo(1)−P(2)	2.531(2)		
Mo(1)−P(3)	2.525(2)		

solution, indicate the presence of metal−sulfur π-bonding in this complex.[6]

In this paper we describe the unusual coordination chemistry of **1**, including the synthesis and structural characterization of an unprecedented edge-shared M_2L_9 complex, $Mo_2(\mu\text{-}S)(\mu\text{-}Cl)Cl_3(PMe_3)_4$ (**2**), containing an open coordination site.[7] The unoccupied site in complex **2** is a source of reactivity, and a variety of ligands can be added to form new M_2L_{10} dimers. However, ligands do not simply add the open site; rather, the stereochemistry of the products is a sensitive function of the electronic and steric properties of the added group. The structural and electronic features of **1** and M_2L_{10} dimers derived from it, and the stability and unusual structure adopted by **2** and related M_2L_9 species, are discussed in terms of metal−metal and metal−ligand multiple bonding effects in the $Mo_2(\mu\text{-}S)(\mu\text{-}X)$ core.

Results

Synthesis and Characterization of $Mo_2(\mu\text{-}S)(\mu\text{-}Cl)Cl_3(PMe_3)_4$ (2). $Mo_2(\mu\text{-}S)(\mu\text{-}Cl)Cl_3(PMe_3)_5$ (**1**) is isolated from reaction 1 as a deep blue-green solid and gives solutions of the same color, but when it is subjected to the repeated addition of benzene or toluene and removal of volatiles, the solution color becomes green and eventually brown. During this workup an equivalent of bound PMe_3 is lost, resulting in the formation of a new dimer, $Mo_2(\mu\text{-}S)(\mu\text{-}Cl)Cl_3(PMe_3)_4$ (**2**) (eq 2). Typically, at least six iterations of solvent addition and removal of the volatiles are required for the reaction to go to completion as determined by ^1H NMR.

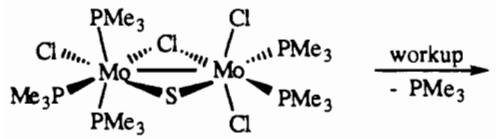

1

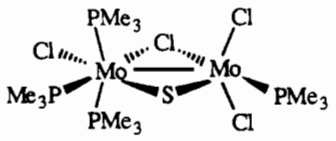

2 (2)

Complex **2** is an air-sensitive dark brown solid, characterized by its ^1H and $^{31}P\{^1H\}$ NMR spectra and an X-ray crystal structure. It is sparingly soluble in benzene and toluene but very soluble in THF and acetone; it is reactive with acetonitrile and methylene chloride (see below). Single crystals of **2**·C_7H_8 were grown by slow diffusion of petroleum ether into a saturated toluene solution of **2** at −12 °C and studied by X-ray diffraction (Tables 1−4). The structure (Figure 1) consists of dimeric molecules with two metals and nine ligands (M_2L_9), very similar to that of **1** except that one of the phosphine ligands is missing. Mo(1) has a distorted octahedral geometry, with three meridonal phosphines, *cis* terminal and bridging chloride ligands, and a bridging sulfido ligand. The configuration and the bond distances and angles are almost identical to those of the analogous half of the M_2L_{10} dimer **1**.[6] The geometry around Mo(2), however, is best described as a trigonal bipyramid with Cl(4), Cl(3), and S(1) in the trigonal plane and P(4) and Cl(1) as the axial ligands. The Cl(3)-Mo(2)-Cl(4), Cl(3)-Mo(2)-S(1), and Cl(4)-Mo(2)-S(1) angles are 124.13(8), 115.11(7), and 115.33(8)°, respectively, and the Cl(1)-Mo(2)-P(4) angle is 166.26(8)° (in contrast, all the angles about octahedral Mo(1) are within ±10° of 90° or ±15° of 180°). Thus, complex **2** is constructed of an octahedron and a trigonal bipyramid fused along a common edge. Such an arrangement is to our knowledge unprecedented for M_2L_9 dimers, which almost without exception adopt a confacial bioctahedral structure, $Y_3M(\mu\text{-}X)_3MY_3$.[2a]

The central $Mo_2(\mu\text{-}S)(\mu\text{-}Cl)$ core is planar (the sum of the interior angles is 359°) and fairly symmetrical, as is typical of this class of dimers (Table 5). The bond distances to Mo(2)

Table 2. Selected Angles (deg) for $Mo_2(\mu\text{-}S)(\mu\text{-}Cl)Cl_3(PMe_3)_4 \cdot C_7H_8$ (**2**·C_7H_8)

Mo(1)−S(1)−Mo(2)	71.31(6)	P(1)−Mo(1)−P(2)	90.53(7)
Mo(1)−Cl(1)−Mo(2)	64.45(5)	P(1)−Mo(1)−P(3)	91.10(7)
Cl(1)−Mo(1)−Cl(2)	85.45(7)	P(2)−Mo(1)−P(3)	165.87(7)
Cl(1)−Mo(1)−S(1)	109.96(7)	Cl(1)−Mo(2)−Cl(3)	89.68(7)
Cl(1)−Mo(1)−P(1)	172.86(7)	Cl(1)−Mo(2)−Cl(4)	90.56(8)
Cl(1)−Mo(1)−P(2)	88.42(7)	Cl(1)−Mo(2)−S(1)	114.29(7)
Cl(1)−Mo(1)−P(3)	88.20(7)	Cl(1)−Mo(2)−P(4)	166.26(8)
Cl(2)−Mo(1)−S(1)	164.59(8)	Cl(3)−Mo(2)−Cl(4)	124.13(8)
Cl(2)−Mo(1)−P(1)	87.41(7)	Cl(3)−Mo(2)−S(1)	115.11(7)
Cl(2)−Mo(1)−P(2)	83.08(7)	Cl(3)−Mo(2)−P(4)	82.87(7)
Cl(2)−Mo(1)−P(3)	82.98(7)	Cl(4)−Mo(2)−S(1)	115.33(8)
S(1)−Mo(1)−P(1)	77.19(7)	Cl(4)−Mo(2)−P(4)	84.16(8)
S(1)−Mo(1)−P(2)	96.72(7)	S(1)−Mo(2)−P(4)	79.40(7)
S(1)−Mo(1)−P(3)	97.33(7)		

Table 3. Positional and Equivalent Isotropic Thermal Parameters for $Mo_2(\mu\text{-}S)(\mu\text{-}Cl)Cl_3(PMe_3)_4 \cdot C_7H_8$ (**2**·C_7H_8)[a]

atom	*x*	*y*	*z*	*B*, Å^2
Mo(1)	0.14133(2)	0.05653(7)	0.26333(3)	2.72(1)
Mo(2)	0.13366(2)	−0.12351(7)	0.34359(3)	2.99(2)
Cl(1)	0.13127(6)	−0.1959(2)	0.23635(9)	4.44(6)
Cl(2)	0.14312(6)	0.0747(3)	0.15398(9)	5.20(6)
Cl(3)	0.19627(6)	−0.2571(3)	0.41948(10)	5.10(6)
Cl(4)	0.06283(6)	−0.2052(3)	0.28855(11)	5.71(7)
S(1)	0.14252(5)	0.1023(2)	0.36537(8)	3.07(5)
P(1)	0.15194(6)	0.3134(2)	0.27699(10)	3.60(5)
P(2)	0.22224(6)	0.0210(3)	0.33081(10)	4.12(6)
P(3)	0.06065(6)	0.0862(3)	0.16826(10)	4.15(6)
P(4)	0.13552(6)	−0.1102(2)	0.45733(9)	3.56(6)
C(1)	0.1121(3)	0.4161(9)	0.2754(4)	5.8(3)
C(2)	0.2004(3)	0.3784(10)	0.3644(4)	6.1(3)
C(3)	0.1559(3)	0.4015(9)	0.2086(4)	6.2(3)
C(4)	0.2485(2)	0.1311(12)	0.3015(4)	7.2(3)
C(5)	0.2573(2)	0.0417(10)	0.4314(4)	5.3(3)
C(6)	0.2380(2)	−0.1466(11)	0.3174(4)	6.5(3)
C(7)	0.0273(2)	0.1312(11)	0.2009(4)	5.6(3)
C(8)	0.0446(3)	0.2156(11)	0.0966(4)	6.1(3)
C(9)	0.0332(3)	−0.0635(10)	0.1106(4)	5.8(3)
C(10)	0.0897(2)	−0.0255(10)	0.4476(4)	5.4(3)
C(11)	0.1834(2)	−0.0294(10)	0.5365(4)	4.8(3)
C(12)	0.1341(2)	−0.2789(10)	0.4918(4)	5.5(3)
C(13)	−0.0811(3)	0.3931(12)	0.0115(5)	9.6(4)
C(14)	−0.0777(3)	0.3882(11)	0.0752(4)	7.5(3)
C(15)	−0.0434(4)	0.4622(13)	0.1378(6)	10.7(5)
C(16)	−0.0163(3)	0.5480(13)	0.1318(6)	9.8(4)
C(17)	−0.0227(4)	0.5458(16)	0.0665(6)	13.1(5)
C(18)	−0.0547(3)	0.4700(11)	0.0039(5)	7.9(3)
C(19)	−0.1144(4)	0.3162(13)	−0.0516(6)	12.1(6)

[a] Anisotropically refined atoms are given in the form of the isotropic equivalent thermal parameter defined as $^4/_3[a^2\beta_{11} + b^2\beta_{22} + c^2\beta_{33} + ab(\cos\gamma)\beta_{12} + ac(\cos\beta)\beta_{13} + bc(\cos\alpha)\beta_{23}]$.

(7) A preliminary account of this work described the syntheses of complexes **2** and **6**: Hall, K. A.; Critchlow, S. C.; Mayer, J. M. *Inorg. Chem.* **1991**, *30*, 3593−3594.

Table 4. Crystallographic Data for Complexes **2**·C_7H_8, **5**[NMe_4], **6**, and **10a**

formula	$Mo_2SCl_4P_4C_{12}H_{36}$·C_7H_8 (**2**)	$Mo_2SCl_5P_4NC_{16}H_{48}$ (**5**)	$Mo_2SCl_4P_4NC_{14}H_{39}$ (**6**)	$Mo_2SCl_4P_4C_{16}H_{42}$ (**10a**)
space group	*C*2/*c* (No. 15)	$P2_1/n$ (No. 14)	$P\bar{1}$ (No. 2)	*Pnma* (No. 62)
unit cell	monoclinic	monoclinic	triclinic	orthorhombic
a, Å	37.822(5)	11.807(1)	8.578(1)	22.166(2)
b, Å	9.6820(9)	16.105(2)	10.176(1)	13.979(1)
c, Å	22.249(3)	17.567(3)	17.562(2)	9.455(1)
α, deg	90	90	101.04(1)	90
β, deg	125.48(1)	98.60(1)	95.54(1)	90
γ, deg	90	90	106.89(1)	90
V, Å^3	6635(3)	3302.8(7)	1420.7(7)	2929.8(4)
Z	8	4	2	4
ϱ_{calcd}, g/cm^3	1.526	1.568	1.662	1.655
fw	762.21	779.6	711.13	730.2
crystal size, mm	0.42 × 0.24 × 0.18	0.20 × 0.25 × 0.35	0.45 × 0.21 × 0.03	0.15 x 0.15 × 0.35
temp, °C	24	22	24	22
μ_{calcd},[a] cm^{-1}	13.24	14.29	15.4	15.15
R[b]	0.043	0.038	0.036	0.027
R_w[b]	0.044	0.054	0.043	0.038
GOF	1.324	1.10	1.114	0.71

[a] An empirical absorption correction was applied; see ref 33. All data collection employed Mo Kα radiation (λ = 0.710 73 Å). [b] $R = \sum||F_o| - |F_c||/\sum|F_o|$; $R_w = [\sum w(|F_o| - |F_c|)^2/\sum wF_o^2]^{1/2}$, where $w^{-1} = [\sigma^2_{count} = (0.06F^2)^2]/4F^2$: Stout, G. H.; Jensen, L. H. *X-Ray Structure Determination*; Wiley: New York, 1989; Chapter 9, p 229, and Chapter 17, p 288.

Table 5. X-ray Data[a] for the $Mo_2(\mu\text{-X})(\mu\text{-Y})$ Cores of the Complexes (X = S, Cl, RS; Y = Cl, RC≡CR, RS)

complex	Mo−Mo	Mo−S	Mo-C_{ac}[b]	C≡C	Mo−Cl_b[b]	Mo−Cl_b−Mo	Mo−S-Mo
$Mo_2(\mu\text{-S})(\mu\text{-Cl})Cl_3(PMe_3)_5$ (**1**)[c]	2.70	2.27, 2.29			2.44	67.1	72.5
$Mo_2(\mu\text{-S})(\mu\text{-Cl})Cl_3(PMe_3)_4$ (**2**)	2.63	2.22, 2.29			2.44, 2.49	64.5	71.3
$Mo_2(\mu\text{-S})(\mu\text{-Cl})Cl_4(PMe_3)_4]NMe_4$ (**5**)	2.68	2.26			2.45, 2.46	66.2	72.8
$Mo_2(\mu\text{-S})(\mu\text{-Cl})Cl_3(PMe_3)_4(CH_3CN)$ (**6**)	2.68	2.25, 2.28			2.45	66.2	72.3
$Mo_2(\mu\text{-S})(\mu\text{-CH}_3C{\equiv}CCH_3)Cl_4(PMe_3)_4$ (**10a**)	2.66	2.25, 2.28	2.14, 2.22	1.36			72.0
$Mo_2(\mu\text{-Cl})_2Cl_4(PMe_2Ph)_4$[d]	2.80				2.38−2.42	71.4, 71.5	
$Mo_2(\mu\text{-Cl})_2Cl_4(PEt_3)_4$[e]	3.73				2.48−2.52	96.4, 96.5	
$Mo_2(\mu\text{-SEt})_2Cl_4(dmpe)_2$[f]	2.71	2.41					67.9[f]
$Mo_2(\mu\text{-S})(\mu\text{-EtC}{\equiv}CEt)(dtc)_3(SCNMe_2)$[g]	2.65	2.26, 2.28	2.11−2.26	1.30			71.2
$Mo_2(\mu\text{-HC}{\equiv}CH)(\mu\text{-O}^i\text{Pr})_2(O^i\text{Pr})_4(py)_2$[h]	2.55		2.07−2.10	1.37			

[a] All bond distances are reported in angstroms and angles in degrees. The estimated errors (Tables 1−3 and 7−15) are typically ≤0.01Å and ≤1°. [b] C_{ac} refers to the acetylenic carbon; Cl_b refers to bridging chloride ligands. [c] The structure of complex **1** is described in ref 6. [d] Reference 18a. [e] Reference 18b. [f] Reference 26. Bond lengths and angles involve SEt^- ligands, not S^{2-}. [g] Reference 8; dtc = dimethyldithiocarbamate, S_2CNMe_2. [h] Reference 20. This complex is a face-shared bioctahedral dimer.

are slightly shorter than those to Mo(1) (Mo(2)−S(1), Mo(1)−S(1) = 2.222(2), 2.288(2) Å; Mo(2)−Cl(1), Mo(1)−Cl(1) = 2.438(2), 2.492(2) Å; compare Mo−S = 2.274(1), 2.285(1) Å and Mo−Cl = 2.436(1), 2.443(1) Å for **1**). In fact, all the bonds to Mo(2) are shorter than the corresponding bonds to Mo(1) and shorter than the corresponding bonds in **1** (except for Mo(2)−Cl(1)). As with complex **1**, the molybdenum−sulfur bonds of **2** fall between those observed for terminal sulfido ligands and most bridging sulfido groups, suggesting the presence of Mo−S multiple bonding.[6] The Mo−Mo distance is 2.629(1) Å, also shorter than that of complex **1** (2.696(1) Å) but within the range of bond lengths observed for other M_2^{6+} molybdenum dimers (2.5−2.8 Å).[2a,8] The chloride and phosphine bond distances to Mo(1) are unexceptional, but those to Mo(2) are slightly shorter than usually encountered.[9]

The central $Mo_2(\mu\text{-S})(\mu\text{-Cl})$ core delineates a pseudomirror plane for the dimer, which also roughly contains P(1) and Cl(2) on Mo(1) and P(4) on Mo(2). For example, the P(1)−Cl(2)−Mo(1) plane is only 0.4° twisted with respect to the core and P(4) lies only 0.06 Å out of the plane of the core. The axial ligands that lie above and below this plane are bent away from each other, with a P(2)-Mo(1)-P(3) "*trans*" angle of 165.87(7)° and a Cl(3)-Mo(2)-Cl(4) angle of only 124.13(8)°. In addition, the nonbonded Cl··CH_3 distances between the axial ligands range from 3.6 to 3.7 Å and are closer to the sum of the van der Waals radii of ca. 3.8 Å[10] than is observed in complex **1** (Cl··CH_3: 3.4−3.6 Å), which has the additional phosphine ligand. Such bending away of axial ligands is typical of ESBO dimers and is thought to relieve significant steric interactions,[2] but the small Cl(3)−Mo(2)−Cl(4) "*trans*" angle is also clearly a result of the lower coordination number of Mo(2) (this angle is within the equatorial plane of the tbp geometry of Mo(2)).

The ^1H and $^{31}P\{^1H\}$ NMR spectra of **2** (Table 6) display a set of three phosphine resonances in a 1:1:2 ratio,[11] consistent with the pseudo-C_s symmetry of the solid state structure. The proton spectrum in C_6D_6 consists of a pair of doublets and a virtual triplet, due to two unique phosphines (P_B and P_C) and the *trans*-equivalent pair of phosphine ligands (P_A), respectively.

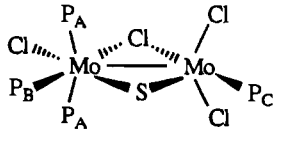

2

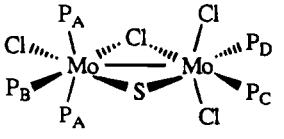

1

Similarly, the $^{31}P\{^1H\}$ spectrum shows a doublet of doublets (J_{PP} = 15, 30 Hz) for the *trans* pair of phosphines P_A and broad

(8) Herrick, R. S.; Nieter-Burgmayer, S. J.; Templeton, J. L. *J. Am. Chem. Soc.* **1983**, *105*, 2599−2605.

(9) Typically, Mo^{III}−Cl distances fall in the range 2.36−2.49 Å while Mo^{III}−P distances range from 2.51−2.60 Å.[6]

(10) *Handbook of Chemistry and Physics*, 54th ed.; Weast, R. C., Ed.; CRC: Boca Raton, FL, 1973−1974; p D-157.

(11) Integration of the $^{31}P\{^1H\}$ NMR spectra reported here give close to integral ratios, indicating that the integrals are not compromised by differential NOE or other effects.

Table 6. ^1H and $^{31}P\{^1H\}$ NMR Data for Complexes **1**−**4** and **7**−**11**[a]

complex	ligand	^1H NMR δ (m, J_{PH} (Hz), no. of H)	$^{31}P\{^1H\}$ NMR δ (m, J_{PP} (Hz), no. of P)
$Mo_2(\mu\text{-}S)(\mu\text{-}Cl)Cl_3(PMe_3)_5$ (**1**)[b]	P_A	0.65 (t, 4, 18H)	−21.9 (d of d, 17 and 37, 2P)
	P_B	1.74 (d, 8, 9H)	−4.4 (t, 37, 1P)
	P_C	1.86 (d, 9, 9H)	10.2 (s, br)
	P_D	1.58 (d, 7, 9H)	−27.4 (s, br, 1P)
$Mo_2(\mu\text{-}S)(\mu\text{-}Cl)Cl_3(PMe_3)_4$ (**2**)[b]	P_A	0.55 (t, 4, 9 H)	−19.7 (d of d, 15 and 31, 2P)
	P_B	1.65 (d, 8, 9H)	1.5 (t, 30, 1P)
	P_C	1.71 (d, 9, 9H)	18.6 (s, br, 1P)
$W_2(\mu\text{-}S)(\mu\text{-}Cl)Cl_3(PMe_3)_4$ (**3b**)[c]	P_A	0.70 (s, br, 18H)	−51.1 (s, br, 2P), $^1J_{WP}$ = 245 Hz
	P_B	1.85 (d, 7, 9H)	−41.0 (s, br, 1P)
	P_C	1.90 (d, 9, 9H)	−5.0 (s, br, 1P)
$Mo_2(\mu\text{-}O)(\mu\text{-}Cl)Cl_3(PMe_3)_4$ (**4b**)[b,c]	P_A	0.71 (t, 3, 18H)	−18.5 (d of d, 12 and 27, 2P)
	P_B	1.45 (d, 9, 9H)	5.0 (s, br, 1P)
	P_C	1.45 (d, 9, 9H)	10.7 (s, br, 1P)
$Mo_2(\mu\text{-}S)(\mu\text{-}Cl)Cl_3(PMe_3)_4(CO)$ (**7**)[b,d]	P_A	0.55 (d, 8, 9H)	−27.2 (d of d, 12 and 31, 1P)
	P_B	1.83 (d, 10, 9H)	10.0 (d, br, 12, 1P)
	P_C	1.64 (d, 9, 9H)	−7.0 (d, 31, 1P)
	P_D	1.53 (d, 8, 9H)	−23.0 (s, br, 1P)
$Mo_2(\mu\text{-}S)(\mu\text{-}Cl)Cl_3(PMe_3)_4(CO)$ (**8a**)[b]	P_A	0.72 (t, 4, 18H)	−19.0 (d, 12, 2P)
	P_B	1.69 (d, 9, 9H)	8.7 (s, br, 1P)
	P_C	1.42 (d, 7, 9H)	−23.0 (s, br, 1P)
$Mo_2(\mu\text{-}S)(\mu\text{-}Cl)Cl_3(PMe_3)_3(CO)$ (**8b**)	P_A	0.59 (t, 4, 18H)	−17.2 (d, 12, 2P)
	P_B	1.55 (d, 10, 9H)	17.4 (t, 12, 1P)
$Mo_2(\mu\text{-}S)(\mu\text{-}RC{\equiv}CR')Cl_4(PMe_3)_4$[e]			
R = H, R′ = CH_3 (**9**)	P_A	0.98 (d, 11, 9H)	2.7 (d, 164, 1P)
	P_A	0.84 (d, 10, 9H)	−3.4 (d of d, 3 and 164, 1P)
	P_B	1.97 (d, 8, 9H)	−12.2 (d, br, 20, 1P)
	P_C	1.56 (d, br, 7, 9H)	−22.9 (d of d, br, 3 and 20 1P)
	R	*f*	
	R′	3.35 (s, 3H)	
R = CH_3, R′ = CH_3 (**10a**)[b]	P_A	0.91 (t, 5, 18H)	−1.5 (d, 4, 2P)
	P_B	2.00 (d, 8, 9H)	−11.9 (d, br, 4, 1P)
	P_C	1.40 (d, 6, 9H)	−25.5 (s, br, 1P)
	R, R′	3.07 (s, 6H)	
R = CH_3, R′ = CH_2CH_3 (**11**)[c,g]	P_A	0.93 (d of d, 3 and 6, 9H)	−3.0 (d of d, 5 and 11, 2P)
	P_A	0.87 (d of d, 3 and 6, 9H)	
	P_B	1.98 (d, 9, 9H)	−1.5 (s, br, 1P)
	P_C	1.61 (d, 6, 9H)	−23.4 (s, br, 1P)
	R	3.18 (s, 3H)	
	R′	1.79 (t, J_{HH} = 8, 3H)	
		3.2−3.7 (m)	
$Mo_2(\mu\text{-}S)(\mu\text{-}CH_3C{\equiv}CCH_3)Cl_4(PMe_3)_3$ (**10b**)	P_A	0.77 (t, 5, 18H)	−7.47 (d, 6, 2P)
	P_B	1.59 (d, 9, 9H)	−4.90 (s, br, 1P)
	CH_3	3.17 (s, 6H)	

[a] All NMR spectra taken in C_6D_6 unless otherwise noted. Assignments of P_A−P_D are given in reference to figures in the text. Integral ratios in the $^{31}P\{^1H\}$ NMR spectra are apparently not compromised by differential NOE or other effects.[11] [b] The ^1H and $^{31}P\{^1H\}$ NMR data have been correlated by $^1H\{^{31}P\}$ NMR experiments. Each ^1H NMR entry corresponds to the $^{31}P\{^1H\}$ NMR entry on the same line. [c] These complexes have been isolated or observed as a part of mixtures (see text and ref 12). [d] Complex **7** was observed during the reaction as a transient species. [e] NMR spectra taken in THF-d_8. [f] The acetylenic proton ($HC{\equiv}CCH_3$) was not found. [g] The ^1H resonances for P_A appear as d of d but are the result of virtual coupling of the methyl protons with each of the phosphorus nuclei. The single $^{31}P\{^1H\}$ resonance for ligands P_A is second order and associated with both ^1H resonances for P_A.

singlet and triplet resonances which become, at −30 °C, sharp triplets with J_{PP} = 14 and 31 Hz, respectively. Presumably the larger coupling constant is the two-bond $^2J_{P_AP_B}$, rather than $^3J_{P_AP_C}$, as is the case in **1**.[6] The resonances of the proton and phosphorus spectra have been correlated by selective $^1H\{^{31}P\}$ NMR data (Table 6) which further support these structural assignments. The pattern and chemical shifts of peaks observed in the spectra of **2** are very similar to those of **1** (Table 6), except for the absence of a doublet (^1H) and a singlet (^{31}P) due to the PMe_3 ligand in **1** which is lost upon conversion to **2** (P_D).

The addition of >1 equivalent of PMe_3 to a dilute solution of **2** results in an immediate color change from gray-green to light blue, and visible spectra of the reaction mixture indicate the conversion of **2** to $Mo_2(\mu\text{-}S)(\mu\text{-}Cl)Cl_3(PMe_3)_5$ (**1**). Subsequent addition of $ZnCl_2$, a phosphine scavenger, causes the solution to change back to gray-green over a period of 1 h with reappearance of the visible spectrum of **2**. These data establish an equilibrium between **1** and **2** + PMe_3 (eq 3).

The addition of PMe_3 to **2** to give **1** can also be followed by NMR (in more concentrated solutions). When both **1** and **2** are present—by adding <1 equiv of PMe_3 to **2**, by removing a portion of the PMe_3 from **1** by trituration and solvent removal, or by mixing isolated samples of **1** and **2**—only one set of resonances intermediate between those of **1** and **2** is seen in the ^1H NMR. As **2** is converted to **1**, the doublet/doublet/triplet ^1H NMR pattern gradually moves toward the chemical shifts characteristic of **1** and the doublet resonance for the added

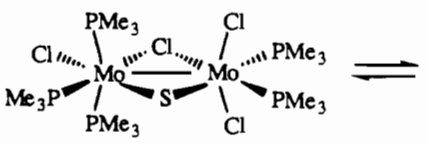

1

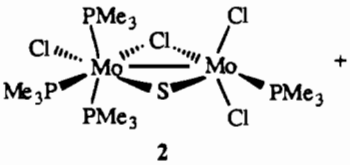

2

+ PMe_3 (3)

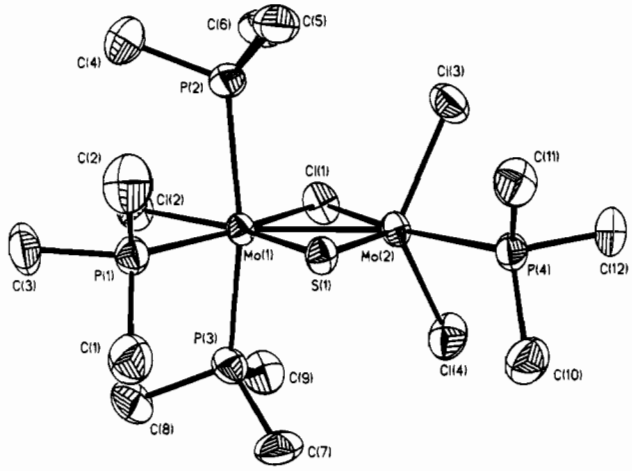

Figure 1. ORTEP drawing of $Mo_2(\mu\text{-}S)(\mu\text{-}Cl)Cl_3(PMe_3)_4$ (**2**)·C_7H_8 showing 40% thermal probability ellipsoids. The hydrogen atoms and toluene solvent molecule have been omitted for clarity.

phosphine ligand grows in. Similar changes are observed in the $^{31}P\{^1H\}$ NMR spectra taken during this process. These data indicate rapid interconversion of **1** and **2** (eq 4). Trace amounts

$$\begin{aligned} &Mo_2(\mu\text{-}S)(\mu\text{-}Cl)Cl_3(PMe_3)_5^{*}\ (\mathbf{1}) \\ &\quad + \quad \rightleftharpoons \\ &Mo_2(\mu\text{-}S)(\mu\text{-}Cl)Cl_3(PMe_3)_4\ (\mathbf{2}) \\ &\qquad\qquad Mo_2(\mu\text{-}S)(\mu\text{-}Cl)Cl_3(PMe_3)_4^{*}\ (\mathbf{2}) \\ &\qquad\qquad\quad + \qquad (4) \\ &\qquad\qquad Mo_2(\mu\text{-}S)(\mu\text{-}Cl)Cl_3(PMe_3)_5\ (\mathbf{1}) \end{aligned}$$

of free PMe_3 likely mediate this equilibration (discussed below), although free PMe_3 is not observed by NMR, at least in part because of the rapid exchange with the fifth phosphine ligand (P_D) in **1**.[6] The broadness seen in spectra of isolated **2** at ambient temperatures may be due to the rate of interconversion of **2** with a small amount of unobserved **1** being close to the NMR time scale.

The interconversion of **1** and **2** most likely occurs by dissociation of P_D from **1**. When PMe_3 is added to solutions of **1**, resonances for P_D and free PMe_3 are not observed in the ^1H NMR spectrum. Rather, the spectra show a broad singlet resulting from coalescence of these signals, suggesting that dissociation/reassociation of P_D is rapid on the NMR time scale. The other phosphine ligands in **1** are considerably less labile, as indicated by an experiment in which **2** was treated with 7 equiv of PMe_3-d_9 to produce **1**. A ^1H NMR spectrum taken after 6 min of reaction showed resonances for P_A, P_B, P_C, and P_D + free PMe_3 in a ratio of 1.2:1:1:0.8, respectively. Since P_A represents two phosphine ligands, this indicates that 40% of these ligands had exchanged with free PMe_3. After 11 min the ratio was 0.8:1:1:1.2, indicating 60% exchange. Spectra taken both 33 and 80 min into the reaction showed the same relative intensities of these peaks: 0.4:1:1:1.6. The constant 0.4:1.6 ratio of P_A to P_D + free PMe_3 is very close to a statistical distribution of 7 deutero phosphines and the 2 protio phosphines initially from P_A ((2/9):(7/9) ≡ 0.44 : 1.56). Thus, the ligands P_A have fully equilibrated with free PMe_3 within 33 min. The intensities of the peaks for P_B and P_C are unchanged over this time scale, indicating slower exchange and no decomposition of **1** under these conditions. After 1 day at ambient temperature, only a small amount (ca. 10−15%) of exchange of protio for deutero phosphine was observed in the sites occupied by P_B and P_C, with a concomitant increase in the intensity of the resonances for P_A and P_D + PMe_3. Thus, the rates of ligand exchange are fastest in the order $P_D \gg P_A \gg P_B \sim P_C$.

The analogous tungsten−sulfido and molybdenum−oxo dimers $W_2(\mu\text{-}S)(\mu\text{-}Cl)Cl_3(PMe_3)_5$ (**3a**) and $Mo_2(\mu\text{-}O)(\mu\text{-}Cl)Cl_3(PMe_3)_5$ (**4a**)[6] also readily lose a phosphine ligand (eq 5).

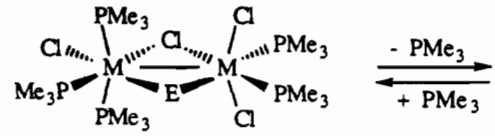

3a, 4a

(5)

3b, 4b

M = W, E = S (**3**); M = Mo, E = O (**4**)

Solutions of these dimers[12a] gradually turn from deep purple to dark green on repeated addition of benzene or toluene and removal of the volatiles. In each instance, the ^1H and $^{31}P\{^1H\}$ NMR spectra (Table 6) suggest loss of 1 equiv of PMe_3 and formation of M_2L_9 dimers analogous to **2**, $W_2(\mu\text{-}S)(\mu\text{-}Cl)Cl_3(PMe_3)_4$ (**3b**) and $Mo_2(\mu\text{-}O)(\mu\text{-}Cl)Cl_3(PMe_3)_4$ (**4b**). Complex **4b** is formed quantitatively from **4a** by NMR, but formation of **3b** is accompanied by other diamagnetic product(s) and insoluble solids; neither has been isolated cleanly.[12b] Addition of a few equivalents of free PMe_3 to solutions of **3b** and **4b** causes an immediate color change from green back to the purple color of **3a** and **4a**, which are observed by ^1H and $^{31}P\{^1H\}$ NMR. This is analogous to the equilibrium interconversion of **1** and **2** + PMe_3 (eq 3).

Reactivity of $Mo_2(\mu\text{-}S)(\mu\text{-}Cl)Cl_3(PMe_3)_4$ (2). The open coordination site in **2** is a source of reactivity, facilitating addition of a variety of ligands to form new M_2L_{10} bioctahedral dimers. Three of these dimers have been structurally characterized; the reaction chemistry is described first, followed by a comparison of the structural data.

Complex **2** reacts readily with chloride ligand sources to give salts of the dark blue $[Mo_2(\mu\text{-}S)(\mu\text{-}Cl)Cl_4(PMe_3)_4]^-$ anion (**5**$^-$, eq 6).

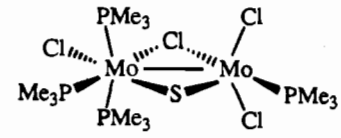

2

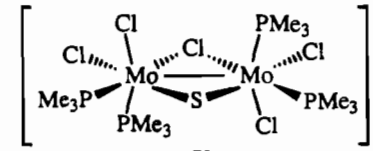

(6)

5$^-$

X-ray quality crystals of **5**[NMe_4] were obtained from reaction of **2** with Me_4NCl in acetone, but the anion is most easily

(12) (a) The complexes $W_2(\mu\text{-}S)(\mu\text{-}Cl)Cl_3(PMe_3)_5$ (**3a**) and $Mo_2(\mu\text{-}O)(\mu\text{-}Cl)Cl_3(PMe_3)_5$ (**4a**) have been isolated as parts of mixtures; see ref 6. (b) Contaminants originally present in **4a** have prevented clean isolation of $Mo_2(\mu\text{-}O)(\mu\text{-}Cl)Cl_3(PMe_3)_4$ (**4b**).[6]

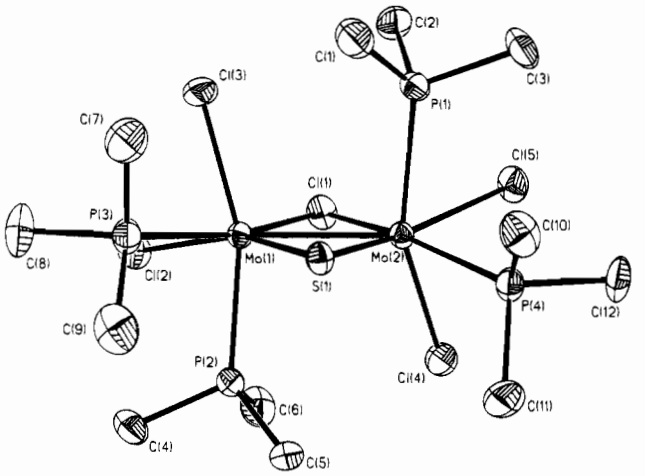

Figure 2. ORTEP drawing of $[Mo_2(\mu\text{-}S)(\mu\text{-}Cl)Cl_4(PMe_3)_4]NMe_4$ (**5**[NMe_4]) showing 40% thermal probability ellipsoids. The hydrogen atoms and $^+NMe_4$ cation have been omitted for clarity.

Table 7. Selected Bond Distances (Å) for $[Mo_2(\mu\text{-}S)(\mu\text{-}Cl)Cl_4(PMe_3)_4]NMe_4$ (**5**)

Mo(1)−Mo(2)	2.684(1)	Mo(2)−Cl(1)	2.462(2)
Mo(1)−Cl(1)	2.453(2)	Mo(2)−Cl(4)	2.485(2)
Mo(1)−Cl(2)	2.530(2)	Mo(2)−Cl(5)	2.561(2)
Mo(1)−Cl(3)	2.468(2)	Mo(2)−S(1)	2.262(2)
Mo(1)−S(1)	2.260(1)	Mo(2)−P(1)	2.519(2)
Mo(1)−P(2)	2.503(2)	Mo(2)−P(4)	2.505(2)
Mo(1)−P(3)	2.522(2)		

Table 8. Selected Angles (deg) for $[Mo_2(\mu\text{-}S)(\mu\text{-}Cl)Cl_4(PMe_3)_4]NMe_4$ (**5**)

Mo(1)−S(1)−Mo(2)	72.8(1)	P(2)−Mo(1)−P(3)	92.8(1)
Mo(1)−Cl(1)−Mo(2)	66.2(1)	Cl(1)−Mo(2)−Cl(4)	87.9(1)
Cl(1)−Mo(1)−Cl(2)	85.8(1)	Cl(1)−Mo(2)−Cl(5)	86.4(1)
Cl(1)−Mo(1)−Cl(3)	87.5(1)	Cl(1)−Mo(2)−S(1)	110.3(1)
Cl(1)−Mo(1)−S(1)	110.7(1)	Cl(1)−Mo(2)−P(1)	96.2(1)
Cl(1)−Mo(1)−P(2)	95.5(1)	Cl(1)−Mo(2)−P(4)	168.3(1)
Cl(1)−Mo(1)−P(3)	168.4(1)	Cl(4)−Mo(2)−Cl(5)	81.7(1)
Cl(2)−Mo(1)−Cl(3)	83.2(1)	Cl(4)−Mo(2)−S(1)	111.4(1)
Cl(2)−Mo(1)−S(1)	159.1(1)	Cl(4)−Mo(2)−P(1)	156.8(1)
Cl(2)−Mo(1)−P(2)	75.7(1)	Cl(4)−Mo(2)−P(4)	80.9(1)
Cl(2)−Mo(1)−P(3)	88.8(1)	Cl(5)−Mo(2)−S(1)	158.6(1)
Cl(3)−Mo(1)−S(1)	109.8(1)	Cl(5)−Mo(2)−P(1)	75.9(1)
Cl(3)−Mo(1)−P(2)	158.4(1)	Cl(5)−Mo(2)−P(4)	88.8(1)
Cl(3)−Mo(1)−P(3)	81.8(1)	S(1)−Mo(2)−P(1)	88.6(1)
S(1)−Mo(1)−P(2)	89.2(1)	S(1)−Mo(2)−P(4)	77.1(1)
S(1)−Mo(1)−P(3)	77.4(1)	P(1)−Mo(2)−P(4)	92.9(1)

isolated as its PPN^+ salt by treating a benzene or toluene suspension of **2** with slightly less than 1 equiv of [PPN]Cl. Complex **5**[PPN] is essentially insoluble in C_6D_6, and deposition is complete after 1 day at 24 °C. The X-ray structure of **5**[NMe_4] (Figure 2, Tables 7−9) shows that a chloride ion occupies what was the open site in **2** (the site occupied by P_D in **1**), as expected. However, a structural rearrangement also occurs, by net exchange of a phosphine on Mo(1) with a chloride on Mo(2). This results in a C_2 symmetric dimer, with two phosphines on each molybdenum, as opposed to the 3:1 pattern in **2**. Rather than a pair of *trans*-equivalent axial phosphines as in **2**, each axial phosphine in **5** is now *trans* to a chloride.

5[PPN] dissolves readily in CH_2Cl_2, but the the NMR spectra of the resulting blue solutions show only resonances for **2** and [PPN]Cl and broad peaks, indicating that **5**[PPN] partially decomposes in solution back to **2**. Consistent with this suggestion, reaction of a faint blue benzene suspension of **5**[PPN] with 3 equiv of PMe_3 for 20 min at 80 °C produced **1** (by NMR) and a stoichiometric amount of [PPN]Cl (isolated and identified by IR; eq 7).

Table 9. Positional and Equivalent Isotropic Thermal Parameters for $[Mo_2(\mu\text{-}S)(\mu\text{-}Cl)Cl_4(PMe_3)_4]NMe_4$ (**5**)[a]

atom	*x*	*y*	*z*	*U*(eq), Å^2
Mo(1)	0.1516(1)	0.2351(1)	0.1731(1)	26(1)
Mo(2)	0.3449(1)	0.2564(1)	0.1122(1)	25(1)
Cl(1)	0.2423(1)	0.1231(1)	0.1091(1)	39(1)
Cl(2)	0.0352(1)	0.1209(1)	0.2230(1)	48(1)
Cl(3)	−0.0057(1)	0.2331(1)	0.0619(1)	49(1)
Cl(4)	0.5023(1)	0.1912(1)	0.2021(1)	45(1)
Cl(5)	0.4561(1)	0.1926(1)	0.0121(1)	46(1)
S(1)	0.2527(1)	0.3541(1)	0.1722(1)	28(1)
P(1)	0.2428(1)	0.3095(1)	−0.0146(1)	34(1)
P(2)	0.2551(1)	0.2050(1)	0.3052(1)	33(1)
P(3)	0.0216(1)	0.3400(1)	0.2224(1)	36(1)
P(4)	0.4840(1)	0.3748(1)	0.1265(1)	33(1)
N(1)	0.7502(4)	0.0516(3)	0.0703(3)	42(2)
C(1)	0.1339(6)	0.3901(5)	−0.0155(4)	53(2)
C(2)	0.1756(6)	0.2294(4)	−0.0790(4)	48(3)
C(3)	0.3342(7)	0.3588(6)	−0.0779(4)	59(3)
C(4)	0.1681(6)	0.2009(5)	0.3821(4)	48(2)
C(5)	0.3671(5)	0.2765(5)	0.3465(4)	44(2)
C(6)	0.3200(7)	0.1025(5)	0.3175(5)	56(3)
C(7)	−0.0408(6)	0.4149(5)	0.1515(5)	61(3)
C(8)	−0.1054(6)	0.2999(6)	0.2543(5)	66(3)
C(9)	0.0766(7)	0.4091(4)	0.3014(5)	57(3)
C(10)	0.4350(6)	0.4779(4)	0.0958(4)	49(2)
C(11)	0.5497(7)	0.3972(5)	0.2232(4)	58(3)
C(12)	0.6103(5)	0.3613(5)	0.0802(4)	51(2)
C(1C)	0.7416(12)	0.0959(8)	−0.0051(6)	114(6)
C(2C)	0.6521(10)	−0.0048(8)	0.0632(10)	133(7)
C(3C)	0.7538(8)	0.1100(9)	0.1282(8)	123(6)
C(4C)	0.8606(7)	0.0072(5)	0.0736(5)	69(3)

[a] Equivalent isotropic *U* defined as one-third of the trace of the orthogonalized U_{ij} tensor.

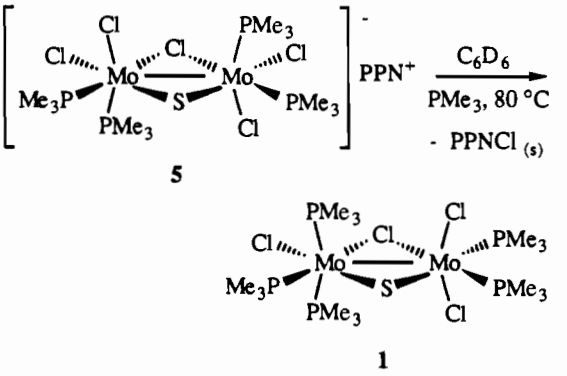

(7)

Complex **2** dissolves in acetonitrile to give a deep blue solution, and slow removal of the volatiles *in vacuo* produces the acetonitrile adduct $Mo_2(\mu\text{-}S)(\mu\text{-}Cl)Cl_3(PMe_3)_4(CH_3CN)$ (**6**) as a dark blue crystalline solid (eq 8).

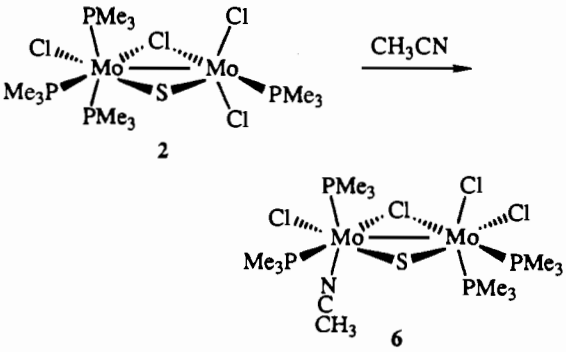

(8)

Complex **6** has been characterized by X-ray crystallography and by a weak infrared absorption at 2260 cm^{-1}, attributed to the $\nu_{C\equiv N}$ of the bound acetonitrile. The structure (Figure 3,

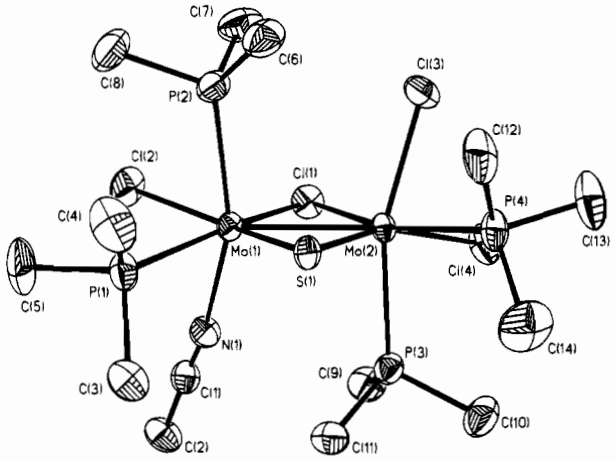

Figure 3. ORTEP drawing of $Mo_2(\mu\text{-}S)(\mu\text{-}Cl)Cl_3(PMe_3)_4(CH_3CN)$ (**6**) showing 40% thermal probability ellipsoids. The hydrogen atoms have been omitted for clarity.

Table 10. Selected Bond Distances (Å) for $Mo_2(\mu\text{-}S)(\mu\text{-}Cl)Cl_3(PMe_3)_4(CH_3CN)$ (**6**)

Mo(1)−Mo(2)	2.6779(6)	Mo(2)−Cl(1)	2.4477(13)
Mo(1)−Cl(1)	2.4532(18)	Mo(2)−Cl(3)	2.4652(17)
Mo(1)−Cl(2)	2.4919(17)	Mo(2)−Cl(4)	2.5142(18)
Mo(1)−S(1)	2.2843(13)	Mo(2)−S(1)	2.2529(16)
Mo(1)−P(1)	2.5085(20)	Mo(2)−P(3)	2.5234(18)
Mo(1)−P(2)	2.4974(18)	Mo(2)−P(4)	2.5317(15)
Mo(1)−N(1)	2.188(5)		

Table 11. Selected Angles (deg) for $Mo_2(\mu\text{-}S)(\mu\text{-}Cl)Cl_3(PMe_3)_4(CH_3CN)$ (**6**)

Mo(1)−S(1)−Mo(2)	72.34(4)	Cl(1)−Mo(2)−Cl(3)	88.35(5)
Mo(1)−Cl(1)−Mo(2)	66.24(4)	Cl(1)−Mo(2)−Cl(4)	85.81(6)
Cl(1)−Mo(1)−Cl(2)	85.84(6)	Cl(1)−Mo(2)−S(1)	111.35(5)
Cl(1)−Mo(1)−S(1)	110.07(5)	Cl(1)−Mo(2)−P(3)	95.23(5)
Cl(1)−Mo(1)−P(1)	168.98(5)	Cl(1)−Mo(2)−P(4)	165.84(6)
Cl(1)−Mo(1)−P(2)	95.07(6)	Cl(3)−Mo(2)−Cl(4)	84.86(6)
Cl(1)−Mo(1)−N(1)	86.30(14)	Cl(3)−Mo(2)−S(1)	108.84(6)
Cl(2)−Mo(1)−S(1)	161.86(6)	Cl(3)−Mo(2)−P(3)	159.80(6)
Cl(2)−Mo(1)−P(1)	87.37(6)	Cl(3)−Mo(2)−P(4)	79.38(6)
Cl(2)−Mo(1)−P(2)	78.36(6)	Cl(4)−Mo(2)−S(1)	157.75(6)
Cl(2)−Mo(1)−N(1)	80.33(13)	Cl(4)−Mo(2)−P(3)	75.62(6)
S(1)−Mo(1)−P(1)	78.11(5)	Cl(4)−Mo(2)−P(4)	86.05(5)
S(1)−Mo(1)−P(2)	91.22(6)	S(1)−Mo(2)−P(3)	88.38(6)
S(1)−Mo(1)−N(1)	108.52(13)	S(1)−Mo(2)−P(4)	79.64(5)
P(1)−Mo(1)−P(2)	92.06(6)	P(3)−Mo(2)−P(4)	93.95(6)
P(1)−Mo(1)−N(1)	84.00(14)	Mo(1)−N(1)−C(1)	170.3(5)
P(2)−Mo(1)−N(1)	158.48(13)		

Tables 10−12) shows that the acetonitrile does not simply fill the open site in **2**; rather, it occupies an axial position. The general arrangement of ligands in **6** is very similar to that of **5**[NMe_4], except that an acetonitrile ligand occupies an axial coordination site instead of a chloride.

Solutions of **6** in CD_3CN give complex ^1H and $^{31}P\{^1H\}$ NMR spectra, which are reproducible but are not easily interpretable (see Experimental Section). Dissolution of the complex in other solvents such as benzene or methylene chloride result in brown solutions and formation of **2** and free CH_3CN, as identified by ^1H and $^{31}P\{^1H\}$ NMR (eq 9). The acetonitrile ligand in **6** is apparently quite weakly bound, so that the complex can only be produced when acetonitrile is present as the solvent. Addition of a few equivalents of PMe_3 to an acetonitrile solution of **6** gives NMR spectra that show the presence of **6** and a set of new resonances very similar to the spectra of **1** in C_6D_6, suggesting that **1** is formed, perhaps in equilibrium amounts.

Benzene or THF solutions of **2** react with carbon monoxide producing a gradual color change from brown to deep blue-green over a period of 2 h and the formation of two carbonyl

Table 12. Positional and Equivalent Isotropic Thermal Parameters for $Mo_2(\mu\text{-}S)(\mu\text{-}Cl)Cl_3(PMe_3)_4(CH_3CN)$ (**6**)[a]

atom	*x*	*y*	*z*	*B*, Å^2
Mo(1)	0.17643(6)	0.16405(5)	0.27123(3)	2.34(1)
Mo(2)	0.30372(6)	0.36662(5)	0.19646(3)	2.20(1)
Cl(1)	0.0137(2)	0.2193(2)	0.16625(9)	3.37(3)
Cl(2)	−0.0924(2)	0.0085(2)	0.29168(11)	4.71(4)
Cl(3)	0.2130(2)	0.5684(2)	0.25366(10)	3.86(4)
Cl(4)	0.2508(2)	0.4345(2)	0.06842(9)	4.13(4)
S(1)	0.4433(2)	0.30938(14)	0.29362(8)	2.48(3)
P(1)	0.3141(2)	0.0592(4)	0.36527(10)	3.41(4)
P(2)	0.1064(2)	0.3219(2)	0.38068(10)	3.48(4)
P(3)	0.4017(2)	0.2047(2)	0.09876(9)	3.21(4)
P(4)	0.5737(2)	0.5666(2)	0.22325(9)	3.21(4)
N(1)	0.1573(6)	−0.0295(5)	0.1859(3)	3.2(1)
C(1)	0.1276(7)	−0.1354(6)	0.1462(4)	3.3(1)
C(2)	0.0888(9)	−0.2733(6)	0.0912(4)	4.5(2)
C(3)	0.4605(9)	−0.0218(7)	0.3267(5)	5.2(2)
C(4)	0.4420(11)	0.1722(7)	0.4569(4)	5.8(2)
C(5)	0.1821(10)	−0.0867(7)	0.3981(5)	6.3(2)
C(6)	0.2617(9)	0.4855(7)	0.4355(7)	4.6(2)
C(7)	−0.0694(9)	0.3763(8)	0.3531(5)	5.3(2)
C(8)	0.0381(10)	0.2430(8)	0.4623(4)	5.5(2)
C(9)	0.2351(9)	0.0850(7)	0.0227(4)	4.6(2)
C(10)	0.5462(9)	0.2866(8)	0.0392(4)	4.9(2)
C(11)	0.5110(8)	0.0946(7)	0.1338(4)	4.2(2)
C(12)	0.6309(9)	0.6617(7)	0.3257(4)	4.9(2)
C(13)	0.5721(10)	0.7031(7)	0.1717(4)	5.7(2)
C(14)	0.7648(9)	0.5374(9)	0.2037(6)	6.7(3)

[a] Anisotropically refined atoms are given in the form of the isotropic equivalent thermal parameter defined as $^4/_3[a^2\beta_{11} + b^2\beta_{22} + c^2\beta_{33} + ab(\cos\gamma)\beta_{12} + ac(\cos\beta)\beta_{13} + bc(\cos\alpha)\beta_{23}]$.

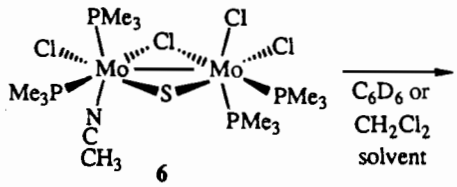

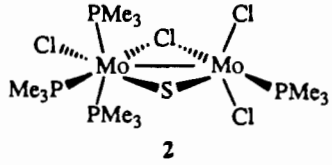

$$+ CH_3CN \quad (9)$$

adducts, **7** and **8a**. Complex **7** is the predominant product during the first couple of hours of the reaction and gradually disappears along with the unreacted **2** to yield complex **8a** cleanly, as determined by NMR and IR. The transient nature of complex **7** has prevented its isolation, and so only **8a** has been isolated. This is most easily accomplished by reacting a concentrated benzene or toluene suspension of **2** with ~1 atm of CO for 1 day, to give a dark blue precipitate of **8a**. Complex **8a** partially decomposes on prolonged exposure to CO (days), resulting in the formation of $SPMe_3$ and uncharacterized diamagnetic carbonyl complexes.

Complexes **7** and **8a** are proposed to be isomers as they each have four phosphine ligands by ^1H and $^{31}P\{^1H\}$ NMR (Table 6) and both have a single CO stretch in their IR spectrum (in C_6D_6: **7**, 1982 cm^{-1}; **8a**, 1942 cm^{-1}). Complex **7** contains four inequivalent phosphine ligands, as indicated by four doublets in the ^1H NMR (integrating 1:1:1:1) and four resonances in the $^{31}P\{^1H\}$ NMR spectrum, two doublets, a doublet of doublets, and a broad singlet, also integrating 1:1:1:1. These data indicate the absence of a *trans*-equivalent pair of phosphines (as in **1** and **2**). Complex **8a**, on the other hand, has phosphine resonances in a 1:1:2 pattern with the largest resonance in the ^1H NMR appearing as a virtual triplet, indicating a *trans*-equivalent phosphine pair and therefore that the single CO ligand

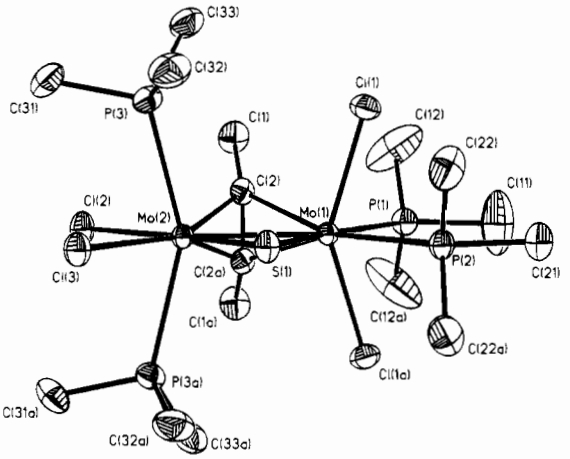

Figure 4. ORTEP drawing of $Mo_2(\mu\text{-}S)(\mu\text{-}CH_3C{\equiv}CCH_3)Cl_4(PMe_3)_4$ (**10a**) showing 40% thermal probability ellipsoids. The hydrogen atoms have been omitted for clarity.

lies in the equatorial (mirror) plane. The $^{31}P\{^1H\}$ resonance for the *trans* phosphines P_A is a doublet with $J_{P_AP_B}$ = 13 Hz, similar to the three-bond couplings across the metal−metal bond in **1** and **2**. These data and other spectral similarities indicate the structure given for **8a**. Consistent with the assignment of

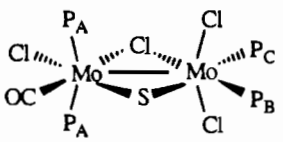

8a

P_C as being *trans* to sulfur, this ligand is labile (see below) and no P_A−P_C coupling is observed. The spectral data for **7** do not uniquely define its stereochemistry but are most consistent with CO coordination at one of the axial sites, again on the basis of a comparison of the chemical shifts and coupling constants for **1** and **2**.

One of the resonances in the phosphorus NMR spectra of **8a** is broad and shows no coupling. On addition of PMe_3 to **8a**, rapid exchange of bound and free phosphine is observed by both ^1H and $^{31}P\{^1H\}$ NMR, and one of the other phosphorus resonances sharpens considerably. This behavior is exactly analogous to that of **1** on addition of PMe_3 and indicates the presence of a single labile phosphine. As with complex **1**, repeated treatment of **8a** with solvent and removal of volatiles causes a color change from blue-green to deep red-brown concomitant with loss of 1 equiv of bound PMe_3. NMR spectra (Table 6) suggest that the new complex formed is $Mo_2(\mu\text{-}S)(\mu\text{-}Cl)Cl_3(PMe_3)_3(CO)$ (**8b**). Moreover, addition of PMe_3 to **8b** regenerates **8a** (eq 10), completely analogous to the interconversion of **1** and **2** (eq 3).

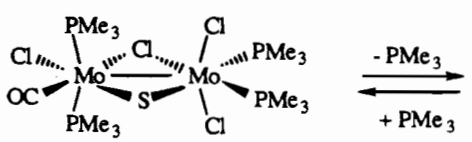

8a

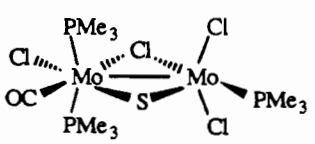

8b (10)

Table 13. Selected Bond Distances(Å) for $Mo_2(\mu\text{-}S)(\mu\text{-}CH_3C{\equiv}CCH_3)Cl_4(PMe_3)_4$ (**10a**)

Mo(2)−Mo(1)	2.661(1)	Mo(1)−S(1)	2.283(2)
Mo(2)−S(1)	2.247(2)	Mo(1)−Cl(1)	2.422(1)
Mo(2)−Cl(2)	2.503(2)	Mo(1)−Cl(1A)	2.422(1)
Mo(2)−Cl(3)	2.550(2)	Mo(1)−P(1)	2.676(2)
Mo(2)−P(3)	2.590(1)	Mo(1)−P(2)	2.627(2)
Mo(2)−P(3A)	2.590(1)	Mo(1)−C(2)	2.217(2)
Mo(2)−C(2)	2.140(4)	Mo(1)−C(2A)	2.217(2)
Mo(2)−C(2A)	2.140(4)	C(2)−C(2A)	1.356(9)
		C(2)−C(1)	1.487(7)

Table 14. Selected Angles (deg) for $Mo_2(\mu\text{-}S)(\mu\text{-}CH_3C{\equiv}CCH_3)Cl_4(PMe_3)_4$ (**10a**)

Mo(1)−S(1)−Mo(2)	72.0(1)	P(3)−Mo(2)−P(3A)	149.0(1)
Mo(1)−C(2)−Mo(2)	75.3(1)	C(2)−Mo(1)−C(2A)	35.6(2)
C(2)−Mo(2)−C(2A)	36.9(2)	C(2)−Mo(1)−P(1)	85.6(1)
C(2)−Mo(2)−Cl(2)	84.3(1)	C(2)−Mo(1)−S(1)	101.5(1)
C(2)−Mo(2)−S(1)	105.1(1)	C(2)−Mo(1)−P(2)	162.1(1)
C(2)−Mo(2)−Cl(3)	159.0(1)	C(2)−Mo(1)−Cl(1)	83.7(1)
C(2)−Mo(2)−P(3)	85.6(1)	C(2)−Mo(1)−Cl(1A)	118.4(1)
C(2)−Mo(2)−P(3A)	122.3(1)	P(1)−Mo(1)−P(2)	96.9(1)
Cl(2)−Mo(2)−Cl(3)	85.9(1)	P(1)−Mo(1)−S(1)	172.6(1)
Cl(2)−Mo(2)−S(1)	170.0(1)	P(1)−Mo(1)−Cl(1)	78.4(1)
Cl(2)−Mo(2)−P(3)	84.8(1)	P(2)−Mo(1)−S(1)	75.7(1)
Cl(3)−Mo(2)−S(1)	84.1(1)	P(2)−Mo(1)−Cl(1)	79.4(1)
Cl(3)−Mo(2)−P(3)	75.1(1)	S(1)−Mo(1)−Cl(1)	99.9(1)
S(1)−Mo(2)−P(3)	92.6(1)	Cl(1)−Mo(1)−Cl(1A)	146.3(1)

The NMR spectra of **8b** are almost identical to that of **8a** (Table 6), differing primarily in the absence of a doublet in the ^1H NMR and a singlet in the $^{31}P\{^1H\}$ NMR. These peaks correspond to the PMe_3 ligand *trans* to the bridging sulfur (P_C), the ligand lost during the workup. A single CO stretch is observed in the IR spectrum at 1944 cm^{-1}. Together, these observations support an edge-shared M_2L_9 structure for **8b** similar to that of **2**.

Complex **2** also reacts with propyne, 2-butyne, or 2-pentyne in benzene or THF for 1 day to give the alkyne adducts $Mo_2(\mu\text{-}S)(\mu\text{-}RC{\equiv}CR')Cl_4(PMe_3)_4$ (RC≡CR′ = $HC{\equiv}CCH_3$ (**9**), $CH_3C{\equiv}CCH_3$ (**10a**), $CH_3C{\equiv}CCH_2CH_3$ (**11**), eq 11). Com-

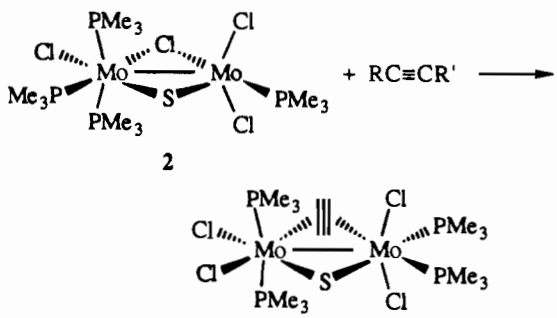

2

(11)

plexes **9** and **10a** are produced cleanly after a few days at 24 °C, but reactions to give **11** do not go to completion. *tert*-Butylacetylene does not produce an analogous adduct, suggesting that the reactions are inhibited by steric bulk.

The acetylene complexes **9**−**11** have been characterized by NMR, and the structure of **10a** has been determined by X-ray crystallography. Crystals of **10a** consist of ESBO dimers (Figure 4, Tables 13−15), like the other products of ligand addition to **2**, but the dimer contains a bridging acetylene rather

than a bridging chloride. There is a crystallographic mirror plane that relates the two axial phosphines (P_A) and the ends of the acetylene. The same structure is adopted in solution, as the axial phosphines appear as a virtual triplet in the ^1H NMR and a doublet in the $^{31}P\{^1H\}$ NMR, and the acetylenic methyl groups give rise to a singlet in the ^1H NMR. The remaining two phosphine ligands appear as doublets (^1H NMR) and a broadened doublet and singlet ($^{31}P\{^1H\}$ NMR).

In complexes **9** and **11**, the different acetylene substituents lead to a slight inequivalence of the *trans* phosphine ligands. In the ^1H NMR these ligands appear as a pair of doublets for **9** and a pair of doublet of doublet resonances for **11**. In the $^{31}P\{^1H\}$ NMR spectrum of **9**, these phosphines appear as a doublet and doublet of doublets which are strongly coupled and slant toward each other considerably. The slanting reflects the fact that the difference in chemical shift between these resonances ($\Delta\nu$ = ~720 Hz) is within an order of magnitude of the P−P coupling constant (J_{PP} = 164 Hz). (The small splitting of the d of d resonance is due to further coupling with an equatorial phosphine.) In **11**, a single doublet of doublets resonance is observed for these two phosphines with apparent "coupling constants" of 5 and 11 Hz, consistent with a second-order ABX pattern.[13] The other coupled phosphine (X) is presumably the PMe_3 ligand *trans* to the alkyne, by analogy to complex **10a** where this $^3J_{PP}$ is 4 Hz.

When $Mo_2(\mu\text{-}S)(\mu\text{-}CH_3C{\equiv}CCH_3)Cl_4(PMe_3)_4$ (**10a**) is subjected to a solvent workup similar to that for **1** and **8a** (eqs 2 and 10), an equivalent of bound PMe_3 is lost resulting in the formation of a new edge-shared M_2L_9 complex, $Mo_2(\mu\text{-}S)(\mu\text{-}CH_3C{\equiv}CCH_3)Cl_4(PMe_3)_3$ (**10b**). Ligand loss in **10a** is reversible, as addition of free PMe_3 to **10b** regenerates **10a**, analogous to complexes **2** and **8b** (eq 12). Complex **10b** gives green

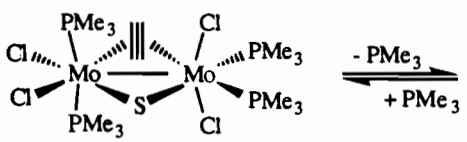

10a

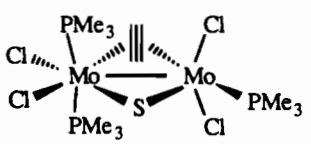

10b (12)

$\|\| \Rightarrow CH_3C{\equiv}CCH_3$

solutions in benzene or toluene and has been identified by its ^1H and $^{31}P\{^1H\}$ NMR spectra (Table 6), which show that the resonances corresponding to one phosphine are absent. It is likely that the phosphine *trans* to sulfur is lost, on the basis of chemical shifts and the somewhat larger structural *trans* influence (see below) and by analogy with compounds **1** and **8a**.

Di-*p*-tolylacetylene reacts with **2** not to form a binuclear adduct but rather to give small amounts of $SPMe_3$ and a monomeric acetylene adduct, $Mo(p\text{-}TolC{\equiv}C\text{-}p\text{-}Tol)Cl_2(PMe_3)_3$ (**12**; eq 13). Only 15% of **2** is converted to **12** after 1 week in THF-d_8, but heating the reaction to 80 °C causes loss of **12**,

(13) Harris, R. K. *Can. J. Chem.* **1964**, *42*, 2275.
(14) (a) Nielson, A. J.; Boyd, P. D. W.; Clark, G. R.; Hunt, T. A.; Metson, J. B.; Rickard, C. E. F; Schwerdtfeger, P. *Polyhedron* **1992**, *11*, 1419. (b) Barrera, J.; Sabat, M.; Harmon, W. D. *Organometallics* **1993**, *12*, 4381−4390.

Table 15. Positional and Equivalent Isotropic Thermal Parameters for $Mo_2(\mu\text{-}S)(\mu\text{-}CH_3C{\equiv}CCH_3)Cl_4(PMe_3)_4$ (**10a**)[a]

atom	*x*	*y*	*z*	*U*(eq), Å^2
Mo(1)	0.2983(1)	0.2500	0.0640(1)	21(1)
Mo(2)	0.4054(1)	0.2500	0.1913(1)	23(1)
Cl(1)	0.2700(1)	0.0842(1)	0.0306(1)	39(1)
Cl(2)	0.5130(1)	0.2500	0.1106(2)	41(1)
Cl(3)	0.4482(1)	0.2500	0.4416(2)	37(1)
S(1)	0.3157(1)	0.2500	0.3020(2)	29(1)
P(1)	0.2627(1)	0.2500	−0.2064(2)	33(1)
P(2)	0.1900(1)	0.2500	0.1772(2)	30(1)
P(3)	0.4244(1)	0.0715(1)	0.2495(1)	34(1)
C(1)	0.4108(2)	0.1307(4)	−0.1217(5)	45(2)
C(2)	0.3867(2)	0.2015(3)	−0.0188(4)	29(1)
C(11)	0.1821(4)	0.2500	−0.2408(10)	105(6)
C(12)	0.2849(5)	0.1505(6)	−0.3142(7)	129(5)
C(21)	0.1214(3)	0.2500	0.0756(8)	49(3)
C(22)	0.1745(2)	0.1496(4)	0.2930(6)	57(2)
C(31)	0.5009(2)	0.0464(4)	0.3069(5)	50(2)
C(32)	0.3778(3)	0.0340(4)	0.3979(6)	56(2)
C(33)	0.4115(3)	−0.0262(3)	0.1255(6)	52(2)

[a] Equivalent isotropic *U* defined as one-third of the trace of the orthogonalized U_{ij} tensor.

$$Mo_2(\mu\text{-}S)(\mu\text{-}Cl)Cl_3(PMe_3)_4 + p\text{-}TolC{\equiv}C\text{-}p\text{-}Tol \rightarrow \underset{\mathbf{2}}{} \underset{\mathbf{12}}{Mo(p\text{-}TolC{\equiv}C\text{-}p\text{-}Tol)Cl_2(PMe_3)_3} + SPMe_3 + \ldots \quad (13)$$

with formation of more $SPMe_3$ and free PMe_3. Presumably, other paramagnetic species are produced because no other species are observed in the NMR and reaction 13 cannot be balanced as written with only 2 equiv of PMe_3 per molybdenum in **2**. Complex **12** is also produced cleanly by reaction of $MoCl_2(PMe_3)_4$ with di-*p*-tolylacetylene (eq 14); analogous tungsten compounds were recently prepared.[14]

$$MoCl_2(PMe_3)_4 + p\text{-}TolC{\equiv}C\text{-}p\text{-}Tol \xrightarrow[80\ ^\circ C]{THF} \underset{\mathbf{12}}{Mo(p\text{-}TolC{\equiv}C\text{-}p\text{-}Tol)Cl_2(PMe_3)_3} + PMe_3 \quad (14)$$

Complex **12** is isolated as a light lime-green solid. Its proton and phosphorus NMR spectra in THF-d_8 display triplet/doublet patterns typical of *mer-cis*-$M(X)Cl_2(PR_3)_3$ compounds.[15] The $^{13}C\{^1H\}$ chemical shift of the acetylenic carbons is 225.3 ppm, similar to that of $W(PhC{\equiv}CPh)Cl_2(PMe_3)_3$ (δ = 228 ppm),[14a] and indicates that the acetylene is a 4-electron donor toward the metal.[16] Complex **12** displays a weak absorption in the IR spectrum at 1620 cm^{-1}, tentatively assigned to the coordinated alkyne, as this value is within the range reported for other 4e$^-$-donating monoalkyne complexes of Mo(II) and W(II) ($\nu_{C\equiv C}$ = 1620−1720 cm^{-1}).[16]

Me_2SO and molecular oxygen both rapidly oxidize complex **2** to form $Mo(O)Cl_2(PMe_3)_3$, $SPMe_3$, and $OPMe_3$ (eq 15).

$$Mo_2(\mu\text{-}S)(\mu\text{-}Cl)Cl_3(PMe_3)_4 + [ox] \rightarrow \underset{\mathbf{2}}{} Mo(O)Cl_2(PMe_3)_3 + SPMe_3 + OPMe_3 + \ldots \quad (15)$$

$$[ox] = Me_2SO, O_2$$

Complex **2** is stable in CH_2Cl_2 for short times but decomposes over a period of days to $MoCl_3(PMe_3)_3$ and $SPMe_3$ along with other paramagnetic species. $Mo(O)Cl_2(PMe_3)_3$, $MoCl_3(PMe_3)_3$,

(15) Hall, K. A.; Mayer, J. M. *J. Am. Chem. Soc.* **1992**, *114*, 10402−10411.
(16) Templeton, J. L. *Adv. Organomet. Chem.* **1988**, *29*, 1−100.

$SPMe_3$, and $OPMe_3$ were identified by comparison of their ^1H and $^{31}P\{^1H\}$ spectra (except $MoCl_3(PMe_3)_3$) with those of authentic samples.[17]

X-ray Structures of 5[NMe4], 6, and 10a. The X-ray structures of $[Mo_2(\mu\text{-}S)(\mu\text{-}Cl)Cl_4(PMe_3)_4]NMe_4$ (**5**[NMe_4]), $Mo_2(\mu\text{-}S)(\mu\text{-}Cl)Cl_3(PMe_3)_4(CH_3CN)$ (**6**), $Mo_2(\mu\text{-}S)(\mu\text{-}CH_3C{\equiv}CCH_3)Cl_4(PMe_3)_4$ (**10a**), and $Mo_2(\mu\text{-}S)(\mu\text{-}Cl)Cl_3(PMe_3)_5$ (**1**)[6] (Figures 2–4; Tables 7–15) show a closely related series of edge-shared bioctahedral (ESBO) dimers, with a remarkable variety of stereochemistries, as noted above. While these are called bioctahedral dimers, the coordination geometries are significantly distorted from regular octahedral geometries, with many of the *trans* angles less than 160°. In **6**, for instance, the *trans* angles between the pairs of axial ligands, P(2)–Mo(1)–N(1) and Cl(3)–Mo(2)–P(3), are 158.48(13) and 159.80(6)°. Such bending of the axial ligands is typical of ESBO structures because of the close contact between these groups.[2a]

Complexes **1**, $\mathbf{5}^-$, and **6** have a central $Mo_2(\mu\text{-}S)(\mu\text{-}Cl)$ core, while in **10a** an acetylene has substituted for the bridging chloride. Complex **2** also has a $Mo_2(\mu\text{-}S)(\mu\text{-}Cl)$ core, but this connects octahedral and trigonal bipyramidal metal centers. A comparison of the metrical data for the core in these and related dimers (Table 5) shows that the shortest Mo–Mo distances are found for the unsaturated complex **2** and then the acetylene-bridged dimer **10a**, but most are in the range 2.63–2.70 Å, consistent with at least a metal–metal single bond.[2a,6,8] The exceptions are the paramagnetic dichloride-bridged dimers $Mo_2(\mu\text{-}Cl)_2Cl_4L_4$ with reduced (L = PMe_2Ph, Mo–Mo = 2.80 Å) or no metal–metal bonding (L = PEt_3, Mo–Mo = 3.73 Å), a distinction that is also apparent in the Mo–Cl–Mo angles.[18] The Mo–S–Mo angles are quite similar for all the dimers at 72.0 ± 0.8°.

The $Mo_2(\mu\text{-}S)(\mu\text{-}Cl)$ cores are all quite symmetrical, with the two Mo–S and Mo–Cl_b distances differing by ≤0.03 Å, except in **2**. The similarity in the bond distances (except for *trans* influences) and the symmetry of the central core suggest that each of the metals in these dimers is in the +3 oxidation state.[6] As noted above, the bond lengths to the five-coordinate molybdenum in **2** (Mo(1)) are significantly shorter than those to the six-coordinate center; for instance, the Mo–S distances differ by 0.07 Å. The $Mo_2(\mu\text{-}S)(\mu\text{-}Cl)$ unit is very close to planar in all the structures. In **1**, this plane roughly defines the equatorial plane of the whole dimer, as the dihedral angle between the $Mo_2(\mu\text{-}S)(\mu\text{-}Cl)$ plane and the planes of the terminal equatorial ligands on Mo(1) and Mo(2) are only 1.3 and 6.6°. Thus, the net twist across the Mo(1)-Mo(2) axis of the dimer is 7.9°, typical of ESBO structures which generally exhibit a twist angle of <10°.[2a] Complexes **5**[NMe_4] and **6**, in contrast, show unusually large twists of 33 and 30°; in **5**[NMe_4], the P(3)–Mo(1)–Cl(2) plane makes a 16° dihedral angle with the plane of the core, which is in turn 17° from the P(4)–Mo(2)–Cl(5) plane (Figure 5).

Complex **10a**, with a bridging acetylene, has no twist across Mo(1)–Mo(2) because it has a crystallographic mirror plane, containing Cl(2), Cl(3), S(1), P(1), and P(2). The central $Mo_2(\mu\text{-}S)(\mu\text{-}CH_3C{\equiv}CCH_3)$ core is somewhat asymmetric, with the sulfido and acetylene ligands closer to Mo(2) (Mo(1)–C(2), Mo(2)–C(2) = 2.217(4), 2.140(4) Å; Mo(1)–S(1), Mo(2)–S(1) = 2.283(2), 2.247(2) Å). The metrical data for the bridging 2-butyne ligand are typical for dinuclear complexes with a perpendicularly bridged acetylene,[19] and the core compares closely with the related d^3–d^3 dimer $Mo_2(\mu\text{-}S)(\mu\text{-}EtC{\equiv}CEt)(S_2CNMe_2)_3(SCNMe_2)$[8] and the face-shared bioctahedral complex $Mo_2(\mu\text{-}HC{\equiv}CH)(\mu\text{-}O^iPr)_2(O^iPr)_4(py)_2$[20] (Table 5).

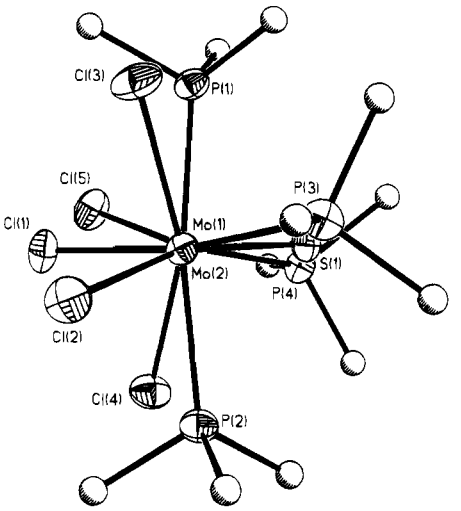

Figure 5. ORTEP drawing of $[Mo_2(\mu\text{-}S)(\mu\text{-}Cl)Cl_4(PMe_3)_4]NMe_4$ (**5**[NMe_4]) viewed down the Mo(1)–Mo(2) axis. The carbon and hydrogen atoms and the $^+NMe_4$ cation have been omitted for clarity.

The Mo-P bond lengths in **1**, **2**, **5**[NMe_4], and **6** are in the range 2.50–2.54 Å, except for bond to the phosphine *trans* to the bridging sulfido in **1**, 2.687(2) Å. Similarly, the Mo-Cl bonds in **1**, **2**, and **6** are 2.41–2.49 Å when not *trans* to sulfur and longer (2.51–2.56 Å) when they are *trans* to sulfur. These data show the significant *trans* influence of the μ-sulfido ligand, consistent with the high lability of phosphines *trans* to sulfur. In general, the bond lengths are slightly shorter in coordinatively unsaturated **2** and slightly longer in the acetylene complex **10a**. In **10a**, both the μ-alkyne and μ-sulfido exhibit significant *trans* influences (e.g., Mo(1)–P(1) = 2.676(2) and Mo(1)–P(2) = 2.627(2) Å; Table 13).

Discussion

Equilibria between M_2L_{10} and M_2L_9 complexes have been studied in considerable detail for d^3–d^3 molybdenum and tungsten systems isoelectronic with **1** and **2** and most recently for d^6–d^6 rhodium dimers.[21] In all previously reported cases, loss of a neutral ligand from an M_2L_{10} edge-shared bioctahedral dimer yields an M_2L_9 *face-shared* bioctahedral (FSBO) species. M_2L_{10}/M_2L_9 edge-shared/face-shared interconversion is typically reversible, and addition of excess ligand often yields M(III) monomeric species, MX_3L_3 (eq 16).

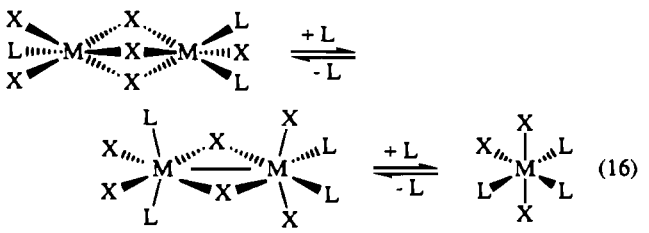

(16)

M = Mo, W, Rh; L = THF, PR_3; X = Cl (also Br for Rh)

In contrast, the structure and facile formation of complex **2**, with its open coordination site, have little precedent in the chemistry of metal dimers. Ligand dissociation from **1**, as indicated by the X-ray structure of **2**, gives not a face-shared

(17) Reference 15 and: (a) $Mo(O)Cl_2(PMe_3)_3$: Carmona, E.; Sanchez, L.; Nielson, A. J.; Wilkinson, G. *Polyhedron* **1984**, *3*, 347–352. (b) $MoCl_3(PMe_3)_3$: Atwood, J. L.; Hunter, W. E.; Carmona-Guzman, E.; Wilkinson, G. *J. Chem. Soc. Dalton Trans.* **1991**, 4550–4554.

(18) (a) Poli, R.; Mui, H. D. *Inorg. Chem.* **1991**, *30*, 65–77. (b) Poli, R.; Mui, H. D. *Inorg. Chem.* **1989**, *28*, 3609.

(19) Hoffman, D. M.; Hoffmann, R.; Fisel, R. *J. Am. Chem. Soc.* **1982**, *104*, 3858.

dimer but an edge-shared species, with a site of unsaturation *trans* to the bridging sulfur. Facile ligand dissociation is also indicated by NMR, including rapid exchange between this phosphine ligand and free PMe_3. Similar NMR properties, and in some cases isolation of M_2L_9 species, indicate that all of the dimers with a phosphine *trans* to sulfur—$M_2(\mu\text{-E})(\mu\text{-Cl})Cl_3(PMe_3)_5$ (M = Mo, W; E = S, O; eqs 2, 3, 5), the carbonyl adduct **8a** (eq 10), and the acetylene adduct **10a** (eq 12)—readily form related unsaturated dimers. And the chloride and acetonitrile adducts $\mathbf{5}^-$ and **6** readily lose the added ligand to reform **2** (e.g., eq 9). This new type of equilibrium between M_2L_{10} and M_2L_9 dimers is general to this class of molecules and is attributable to the presence of a bridging sulfido or oxo ligand. Moreover, the μ-S or μ-O ligand prevents dissociation of the M_2L_{10} dimers to M(III) monomers upon addition of free PMe_3 (cf. eq 16) because of the instability of d^3 terminal sulfido and oxo complexes.[22]

The labile phosphine ligands *trans* to sulfur or oxygen dissociate very rapidly, as indicated by fast exchange with free PMe_3 on the NMR time scale.[23] The separation between bound and free PMe_3 resonances in the $^{31}P\{^1H\}$ NMR is 2700–5000 Hz for compounds **1**, **3a**,[6] **4a**,[6] **8a**, and **10a** (determined in the absence of free PMe_3), which indicates that the rate constants for ligand exchange are $\geq 10^5$ s^{-1}.[24] This is at least 10^7 times faster than the exchange observed at the *trans* axial sites P_A in **1** ($6 \leq t_{1/2} \leq 11$ min). The other two phosphine ligands, P_B and P_C, which lie *trans* to the bridging chloride, are essentially substitution inert. The remarkable difference in lability of the phosphine ligands in **1** indicates a kinetic *trans* effect in the order S > P > Cl_b. This parallels the structural *trans* influence on the Mo–P bond distances which are longest for phosphine ligands *trans* to ligands in the order S > P > Cl_b. The greater *trans*-labilizing ability of phosphine versus a bridging chloride has also been noted in $Mo_2(\mu\text{-Cl})_2Cl_4(PMe_3)_4$[21f] as well as in reactions of the monomeric Mo(III) complex $MoCl_3(THF)_3$ with phosphines.[21d] The *trans* influence of the bridging sulfido and oxo is reminiscent of the strong *trans* influence seen in monomeric complexes with terminal oxo and sulfido ligands.[4b]

In forming adducts with complex **2**, the various substrates are observed to occupy a number of different sites:

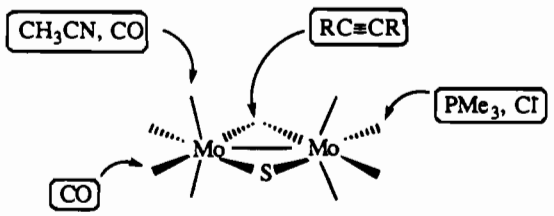

Only in the case of addition of PMe_3 to form **1** does ligand association occur by simple addition to the open equatorial coordination site of **2**, without any rearrangement of the other ligands. CH_3CN takes the place of a *trans* axial PMe_3 ligand, and the resulting structure of **6** has axial phosphines on different molybdenum centers and a chloride occupying what was the open site. Chloride addition gives a similar structure ($\mathbf{5}^-$) with axial phosphines on different molybdenum centers; it is not clear whether the added chloride occupies an equatorial site (as in PMe_3 addition) or an axial site (similar to CH_3CN) but there is a net gain of one equatorial chloride ligand. From NMR data, carbon monoxide binds in two different positions, apparently as an axial ligand initially and eventually in a more thermodynamically preferred equatorial position *trans* to the bridging chloride. Acetylenes bind as bridging ligands, which moves a chloride ligand to a terminal position and redistributes the phosphines so that there are two on each molybdenum, rather than the 3:1 pattern in **2**.

It is perhaps surprising that ligands do not simply bind to the open site, but substitution of an axial phosphine is reasonable, given the lability of these positions in **1**. In all cases except the initial CO adduct **7**, the products are most likely the thermodynamically most stable isomers. The affinity of acetylenes to be bridging ligands, due to their orthogonal pair of π orbitals, is well documented.[19] In general, two phosphine ligands never appear in axial positions *cis* across the metal–metal bond, presumably for steric reasons (as has been previously noted for M_2L_{10} dimers[2a]). There also appears to be a preference for chloride *trans* to the bridging sulfur rather than PMe_3, as all the structures contain at least one chloride ligand in this position. (A similar preference for hard ligands *trans* to a terminal oxo has been noted,[25] and this would appear to apply to terminal sulfido compounds as well.) Both these preferences are accommodated in the chloride and acetonitrile addition products $\mathbf{5}^-$ and **6**. But with five phosphine ligands, as in **1**, or with CO occupying an equatorial site as in **8a**, one phosphine must occupy the site *trans* to the bridging sulfur in order to avoid *cis* axial interactions across the metal–metal bond—and this phosphine is very labile.

The $Mo_2(\mu\text{-S})(\mu\text{-Cl})$ core is maintained in most of the reactions of **2** and is quite insensitive to differences in the ligand environments and to the twisting distortions about the metal–metal axis observed in $\mathbf{5}[NMe_4]$ and **6**. The importance of the sulfido ligand in the apparent stability of this core is illustrated by the comparison between **1** and analogs with two bridging chlorides or two bridging thiolates: $Mo_2(\mu\text{-Cl})_2Cl_4(PR_3)_4$[18,21f] and $Mo_2(\mu\text{-SEt})_2Cl_4(dmpe)_2$ (dmpe = $Me_2PCH_2CH_2PMe_2$)$_2$.[26] These compounds are d^3–d^3 Mo_2L_{10} ESBO dimers and are isoelectronic with **1**, differing in the replacement of the sulfido and a phosphine in **1** by two chlorides or two thiolates. However, **1** is diamagnetic while $Mo_2(\mu\text{-Cl})_2Cl_4(PMe_3)_4$ and $Mo_2(\mu\text{-SEt})_2Cl_4(dmpe)_2$ are paramagnetic, and as noted earlier (eq 16), loss of a phosphine ligand from the $Mo_2(\mu\text{-Cl})_2Cl_4(PMe_3)_4$ gives the face-shared M_2L_9 complex $Mo_2(\mu\text{-Cl})_3Cl_3(PMe_3)_3$ rather than an edge-shared dimer such as **2**.[21f] The

(20) Chisholm, M. H.; Huffman, J. C.; Rothwell, I. P. *J. Am. Chem. Soc.* **1981**, *103*, 4245.

(21) Reference 18 and: (a) Owens, B. E.; Poli, R. *Polyhedron* **1989**, *8*, 545–548. (b) Chacon, S. T.; Chisholm, M. H.; Streib, W. E.; Van Der Sluys, W. *Inorg. Chem.* **1989**, *28*, 6–8. (c) Poli, R.; Mui, H. D. *J. Am. Chem. Soc.* **1990**, *112*, 2446–2448. (d) Poli, R.; Gordon, J. C. *Inorg. Chem.* **1991**, *30*, 4550–4554. (e) Gordon, J. C.; Mui, H. D.; Poli, R.; Ahmed, K. T. *Polyhedron* **1991**, *10*, 1667–1674. (f) Poli, R.; Gordon, J. C. *J. Am. Chem. Soc.* **1992**, *114*, 6723–6734. (g) Poli, R. *Comments Inorg. Chem.* **1992**, *12*, 285. (h) Barry, J. T.; Chacon, S. T.; Chisholm, M. H.; DiStasi, V. F.; Huffman, J. C.; Streib, W. E.; Van Der Sluys, W. *Inorg. Chem.* **1993**, *32*, 2322–2331. (i) Cotton, F. A.; Eglin, J. L.; Kang, S.-J. *Inorg. Chem.* **1993**, *32*, 2332–2335. (j) Cotton, F. A.; Kang, S.-J. *Inorg. Chem.* **1993**, *32*, 2336–2342. (k) Rothfuss, H.; Barry, J. T.; Huffman, J. C.; Caulton, K. G.; Chisholm, M. H. *Inorg. Chem.* **1993**, *32*, 4573–4577.

(22) Mayer, J. M. *Comments Inorg. Chem.* **1990**, *29*, 4862–4867. This is discussed in more detail in ref 6.

(23) The mechanism for ligand exchange almost certainly involves a first-order dissociation from the M_2L_{10} complex, followed by reassociation of free PMe_3. The observation that M_2L_{10} and M_2L_9 rapidly interconvert in the absence of free PMe_3 argues against associative pathways.

(24) Observation of a single coalesced line requires $k \geq \pi\Delta\nu/\sqrt{2}$: Crabtree, R. *The Organometallic Chemistry of the Transition Metals*; Wiley-Interscience: New York, 1988; Chapter 10, pp 213–214. Drago, R. S. *Physical Methods in Chemistry*; Saunders College Publishing: Chicago, 1977; Chapter 7, p 223.

(25) Bryan, J. C.; Stenkamp, R. E.; Tulip, T. H.; Mayer, J. M. *Inorg. Chem.* **1987**, *26*, 2283-2288.

(26) Cotton, F. A.; Diebold, M. P.; O'Connor, C. J.; Powell, G. L. *J. Am. Chem. Soc.* **1985**, *107*, 7438.

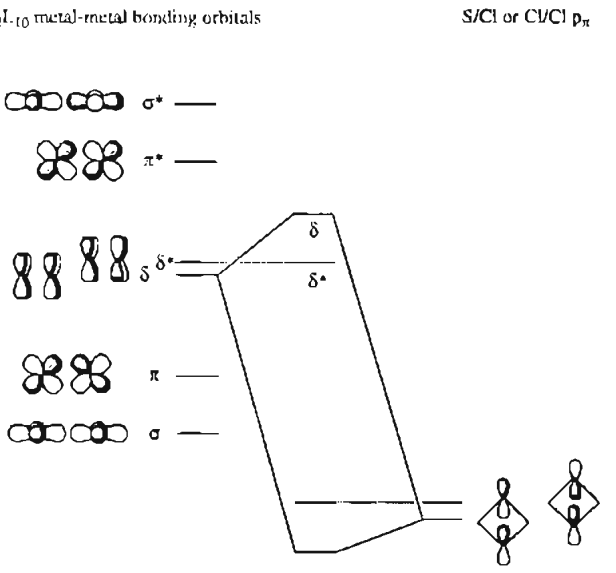

Figure 6. Schematic orbital interactions in M_2L_{10} complexes (adapted from ref 2a).

differences in these systems can be understood in terms of the electronic interactions within the cores, $Mo_2(\mu\text{-S})(\mu\text{-Cl})$ versus $Mo_2(\mu\text{-Cl})_2$ and $Mo_2(\mu\text{-SEt})_2$.

A number of theoretical studies of edge-shared bioctahedral dimers paint a consistent picture of the metal−metal and metal−bridging ligand interactions.[27] Each of the octahedral metal centers has three t_{2g}-like orbitals that are not involved in σ bonding, and these interact in the dimers to make metal-metal σ, π, and δ bonding and antibonding orbitals (Figure 6). In d^3−d^3 dimers, the σ and π bonding orbitals are filled and the δ and δ^* orbitals are typically quite close in energy.[27] The π-donor orbitals of the bridging ligands, S and Cl filled p orbitals in this case, interact with the metal−metal π and δ bonding orbitals (Figure 6 shows only the δ orbital interaction), thus creating a splitting between the δ and δ^* orbitals.[27] The difference between the $Mo_2(\mu\text{-S})(\mu\text{-Cl})$ core versus $Mo_2(\mu\text{-Cl})_2$ and $Mo_2(\mu\text{-SEt})_2$ is the magnitude of this splitting. With poorer π donors, such as μ-Cl and μ-SR ligands, this splitting is small and the $\sigma^2\pi^2\delta^{*1}\delta^1$ triplet state is thermally populated and accounts for the magnetic properties of these materials.[27] μ-Sulfido and μ-oxo ligands, however, are strong π donors and should cause a significantly larger δ−δ^* splitting, consistent with the diamagnetic ($\sigma^2\pi^2\delta^{*2}$) ground states observed for all the compounds discussed here. The electronic effect of the strong π-donating sulfur or oxygen is reminiscent of that observed in mononuclear octahedral d^2 complexes, which are paramagnetic unless a π-donor ligand is present.[4h,28]

The electronic picture depicted for complex **1** and the adducts of **2** suggests a bond order between 1 and 2 for the metal−metal bond (depending on the antibonding character of the δ^*) and a bond order of 1.5 for the Mo−S bonds, consistent with the metrical data. The strong Mo−S bonding is likely the origin of the *trans* effect and *trans* influence of the μ-sulfido ligand. In the μ-alkyne complexes **9**−**11**, the sulfur is responsible for all of the metal−bridge π bonding of the type shown in Figure 6, as the alkyne has no accessible orbital of the right symmetry.[29] The similarity of the Mo−S distances in **1**, **5**[NMe_4], **6**, and **10a** reinforces the suggestion that π-donation from sulfur is much more important than that from a bridging chloride. The preference of the alkyne ligands for a bridging site, in the $\pi_\perp$ orientation, is likely due both to the ability of an alkyne to be a strong σ donor to two metals and to its π-acceptor capability, which should stabilize the metal-metal δ^* and π orbitals.[19]

The unusual stability of **2**, with its open coordination site, may be the result of the strong Mo-S π bonding. It is not unreasonable that metal−bridge π bonding would be stronger in an edge-shared bioctahedral dimer than in the alternative face-shared structure, in which there is extensive mixing of the metal−ligand σ and π interactions.[29] However, this must be a tentative suggestion because this mixing of metal−metal and various metal−ligand interactions leads to complicated orbital pictures for face-shared bioctahedral complexes,[20] from which the effect of one interaction such as Mo-S π bonding is difficult to extract.

Experimental Section

General Considerations. All experiments were performed under a nitrogen or argon atmosphere or under vacuum employing high vacuum line or Schlenk techniques and a glovebox. Solvents were dried according to standard procedures.[30] All reagents were degassed on the vacuum line, checked for purity by NMR, and if necessary dried by standard means, except gases, which were used directly from the cylinder without further purification. Deuterated solvents were purchased from Cambridge Isotope Laboratories. All gases were purchased from Matheson. All acetylenes, DMSO, PMe_3 (Aldrich), and $SPMe_3$ (Alfa) were degassed (where applicable) and used without further purification. The following compounds were previously reported: $MoCl_2(PMe_3)_4$,[31] $Mo(O)Cl_2(PMe_3)_3$,[15,17a] $MoCl_3(PMe_3)_3$,[17b] $Mo_2(\mu\text{-S})(\mu\text{-Cl})Cl_2(PMe_3)_5$ (**1**),[6] $W_2(\mu\text{-S})(\mu\text{-Cl})Cl_4(PMe_3)_5$ (**3a**),[6,12] and $Mo_2(\mu\text{-O})(\mu\text{-Cl})Cl_2(PMe_3)_6$ (**4a**).[6,12] PMe_3-d_9 was prepared according to published procedures.[32]

NMR spectra were acquired at ambient temperatures (24 ± 2 °C) unless otherwise noted using Bruker WM-500, AF-300, and AC-200 and Varian VXR-300 Fourier transform spectrometers. NMR data are reported in Table 6 unless otherwise noted. The ^{1}H NMR were referenced to TMS, or the residual protons of the solvent. The ^{31}P{^{1}H} NMR spectra were recorded at 202.5, 121.4, or 80.0 MHz and were referenced to external 85% H_3PO_4. The ^{13}C{^{1}H} NMR spectra were recorded at 75.43 MHz and referenced relative to C_6D_6 (δ 128 ppm). Spectra are reported as δ (ppm) (number of hydrogens, multiplicity, coupling constants (Hz), assignment). Infrared spectra were recorded on a Perkin-Elmer 1604 FTIR as Nujol mulls or in solutions using NaCl plates and are reported in cm^{-1}. Intensities of IR bands are given as (s) = strong, (m) = medium, (w) = weak, or (sh) = shoulder. UV−vis spectra were taken on a Hewlett Packard 8450 ultraviolet/visible spectrometer.

Many of the reactions studied were performed in sealed NMR tubes. In a typical procedure, an NMR tube sealed to a ground glass joint is charged with reagents and solvent in the drybox and then fitted with a Teflon needle valve. The contents of the tube are degassed on the

(27) References 2a, 5, 18, and 26 and: (a) Shaik, S.; Hoffmann, R.; Fisel, C. R.; Summerville, R. H. *J. Am. Chem. Soc.* **1980**, *102*, 4555. (b) Anderson, L. B.; Cotton, F. A.; De Marco, D.; Fang, A.; Ilsley, W. H.; Kolthammer, W. S.; Walton, R. A. *J. Am. Chem. Soc.* **1981**, *103*, 5078. (c) Chakavorty, A. R.; Cotton, F. A.; Diebold, M. P.; Lewis, D. B.; Roth, W. J. *J. Am. Chem. Soc.* **1986**, *108*, 971. (d) Poh, R.; Torralba, R. C. *Inorg. Chim. Acta* **1993**, *212*, 123.

(28) Over, D. E.; Critchlow, S. C.; Mayer, J. M. *Inorg. Chem.* **1992**, *31*, 4643−4648.

(29) (a) Saillant, R.; Wentworth, R. A. D. *J. Am. Chem. Soc.* **1969**, *91*, 2174. (b) Templeton, J. L.; Jacobsen, R. A.; McCarley, R. E. *Inorg. Chem.* **1977**, *16*, 3320. (c) Templeton, J. L.; Dorman, W. C.; Clardy, J. E.; McCarley, R. E. *Inorg. Chem.* **1978**, *17*, 1263. (d) Summerville, R. H.; Hoffmann, R. *J. Am. Chem. Soc.* **1979**, *101*, 3821 and references therein.

(30) Perrin, D. D.; Armarego, W. L. F. *Purification of Laboratory Chemicals*, 3rd ed.; Pergamon: New York, 1989.

(31) Reference 15 and: Rodgers, R. D.; Carmona, E.; Galindo, A.; Atwood, J. L.; Canada, L. G. *J. Organomet. Chem.* **1984**, *277*, 403−415.

(32) Leutkens, M. L., Jr.; Elcesser, W. L.; Huffman, J. C.; Sattelberger, A. P. *Inorg. Chem.* **1984**, *23*, 1718−1726.

vacuum line, and additional reagents are added if required. The contents of the tube are then frozen at −196 °C, and the tube is sealed with a torch. The tube is then thawed by rinsing it with acetone, and subsequent reactions are followed by NMR.

$Mo_2(\mu\text{-}S)(\mu\text{-}Cl)Cl_3(PMe_3)_4$ (2). A solution of **1** (1.5 g, 2.0 mmol) dissolved in 50 mL of toluene was stirred briefly and stripped of volatiles under vacuum. The solids were repeatedly dissolved in fresh toluene and stripped until the original blue-green color of the solution became brown, yielding **2** as a brown solid, which was scraped from the walls of the flask (1.2 g, 90%). Typically at least six iterations are required for complete conversion to **2** as determined by ^1H and $^{31}P\{^1H\}$ NMR. Recrystallization is best achieved by allowing petroleum ether to slowly diffuse into a saturated toluene solution of **2**. ^1H and $^{31}P\{^1H\}$ NMR (at ambient temperature in C_6D_6): see Table 6. $^{31}P\{^1H\}$ NMR (at −30 °C in CD_2Cl_2): 25.4 (1P, t, J_{PP} = 14 Hz, *cis*-$P(CH_3)_3$), 6.9 (1P, t, J_{PP} = 31 Hz, *cis*-$P(CH_3)_3$), −18.5 (2P, d of d, J_{PP} = 14, 31 Hz, *trans*-$P(CH_3)_3$). IR (Nujol) 1416 (w), 1299 (s), 1280 (s), 948 (s), 846 (w), 668 (sh). UV/vis (λ, nm (ϵ)): 308 (sh, 6000), 470 (3000), 582 (1600), 720 (1400). Anal. Calcd for $Mo_2SCl_4P_4C_{12}H_{36}$: C, 21.51; H, 5.42. Found: C, 21.30; H, 5.42.

$W_2(\mu\text{-}S)(\mu\text{-}Cl)Cl_3(PMe_3)_4$ (3b). A solution of **3a** (15 mg, 1.6 × 10^{-2} mmol) in 0.5 mL of benzene was strirred briefly, and then the volatiles were removed. The solids were repeatedly dissolved in toluene and stripped to give a dark green-brown solid containing complex **3b** along with unidentified diamagnetic product(s) by ^1H and $^{31}P\{^1H\}$ NMR. Addition of PMe_3 to the solids converted **3b** back to **3a** but did not have a similar reversing effect on the other species.

$Mo_2(\mu\text{-}O)(\mu\text{-}Cl)Cl_3(PMe_3)_4$ (4b). Complex **4b** was detected by ^1H and $^{31}P\{^1H\}$ NMR when a sample of **4a** was dissolved in toluene and stripped of volatiles six times. Addition of a few equivalents of PMe_3 to the dark green solids regenerated **4a** cleanly (by NMR).

$[Mo_2(\mu\text{-}S)(\mu\text{-}Cl)Cl_4(PMe_3)_4]^-$. 5[NMe4]. In an NMR tube, a brown suspension containing 10 mg (1.5 × 10^{-2} mmol) of **2**, 8 mg (7.5 × 10^{-2} mmol) of Me_4NCl, and 0.5 mL of acetone-d_6 was prepared. The suspension over a period of 50 min became deep blue and after a few days deposited large crystals of **5**[NMe_4], suitable for X-ray analysis.

5[PPN]. Stirring a suspension of **2** (50 mg, 7.5 × 10^{-2} mmol), [PPN]Cl (39 mg, 6.7 × 10^{-2} mmol; 0.9 equiv), and 4 mL of toluene for 1.5 days caused a color change to deep blue and deposited dark blue crystalline solids. The solids were filtered off, washed with 3 × 1 mL of toluene, and dried *in vacuo*, yielding 60 mg (90% based on [PPN]Cl). The complex crystallizes with 1 equiv of toluene, as indicated by elemental analysis and the observation of 1 equiv of C_7H_8 by NMR on heating **5**[PPN]·C_7H_8 with PMe_3 in C_6D_6. **5**[PPN] is best recrystallized by slow diffusion of diethyl ether into a saturated CH_2Cl_2 solution of the complex at −40 °C. IR (Nujol): 1438 (sh), 1366 (sh), 1294 (m), 1272 (s), 1183 (w), 1166 (w), 1114 (s), 996 (w), 949 (s), 891 (w), 849 (w), 748 (sh), 692 (m), 668 (w). Anal. Calcd for **5**[PPN]·C_7H_8, $Mo_2SCl_5P_6NC_{55}H_{74}$: C, 49.44; H, 5.58; N, 1.05. Found: (average of two analyses): C, 50.00; H, 5.61; N, 1.55.

$Mo_2(\mu\text{-}S)(\mu\text{-}Cl)Cl_3(PMe_3)_4(CH_3CN)$ (6). A solution of **2** (75 mg, 0.11 mmol) in 15 mL of CH_3CN was stirred for 0.5 h, and the volatiles were slowly removed under vacuum, causing crystallization of **6** as a dark navy blue solid. Yield: 72 mg (90%) Complex **6** is unstable in CH_2Cl_2, benzene, and toluene, decomposing to **2** and free CH_3CN. ^1H NMR (CD_3CN): 1.8−2.0 (multiplets), 0.7 (broad hump), 0.54 (t, J_{PH} = 3 Hz). $^{31}P\{^1H\}$ NMR: 2.0, 5.0, 8.5 (broad humps). The broad resonances sharpen into complex multiplets at −45 °C; the low-temperature $^{31}P\{^1H\}$ spectra appear to be second order. IR (Nujol): 2260 (w, ν_{CN}), 1416 (w), 1299 (w), 1277 (s), 947 (s), 847 (w), 669 (sh). Anal. Calcd for $Mo_2SCl_4P_4NC_{14}H_{39}$: C, 23.65; H, 5.53; N, 1.97. Found: C, 23.72; H, 5.46; N, 2.16.

$Mo_2(\mu\text{-}S)(\mu\text{-}Cl)Cl_3(PMe_3)_4(CO)$ (7). Complex **7** was detected as a transient species by ^1H and $^{31}P\{^1H\}$ NMR and IR when a suspension of **2** (10 mg; 1.5 × 10^{-2} mmol) in 0.5 mL of C_6D_6 was allowed to react with ~1 atm of CO for ~1 h in a sealed NMR tube. IR (C_6D_6): ν_{CO} = 1982 cm^{-1}.

$Mo_2(\mu\text{-}S)(\mu\text{-}Cl)Cl_3(PMe_3)_4(CO)$ (8a). A 26 mL glass-walled reaction bomb was charged with 200 mg of **2** (0.3 mmol), 8 mL of benzene, and 1 atm of CO. Stirring for 3 days caused a color change to deep blue and deposited dark blue crystals of **8a** (50 mg). The filtrate was layered with ~2 mL of ether and allowed to stand overnight, depositing 96 mg more of crystals of **8a**, for a total yield of 146 mg (70%). Complex **8a** is unstable to repeated solvent exposure, losing an equivalent of bound PMe_3 to form **8b** (see below), but this is reversible, so **8a** may be regenerated by recrystallization in the presence of a small amount of PMe_3. IR (Nujol): 1928 (s, ν_{CO}), 1455 (sh), 1435 (sh), 1417 (w), 1299 (w), 1278 (m), 1153 (m), 1140 (m), 952 (s), 849 (w), 736 (sh), 689 (w). Anal. Calcd for $Mo_2SCl_4P_4OC_{13}H_{36}$: C, 22.37; H, 5.20. Found: C, 22.23; H, 5.15.

$Mo_2(\mu\text{-}S)(\mu\text{-}Cl)Cl_3(PMe_3)_3(CO)$ (8b). Complex **8b** was detected in high yield (>95%) by NMR when 15 mg (2.1 × 10^{-2} mmol) of **8a** was repeatedly dissolved in 2 mL benzene and stripped of volatiles 12 times, to give a dark brown residue. IR (C_6D_6): ν_{CO} = 1944 cm^{-1}.

$Mo_2(\mu\text{-}S)(\mu\text{-}HC{\equiv}CCH_3)Cl_4(PMe_3)_4$ (9). Complex **9** was detected in >90%yield by NMR when a C_6D_6 suspension of **2** (10 mg; 1.5 × 10^{-2} mmol) was reacted with 4.5 × 10^{-2} mmol of propyne for 2 days.

$Mo_2(\mu\text{-}S)(\mu\text{-}CH_3C{\equiv}CCH_3)Cl_4(PMe_3)_4$ (10a). A solution of **2** (200 mg, 0.3 mmol) and 2-butyne (0.6 mmol, added by gas addition) in 8 mL of benzene was stirred for 2 days, depositing **10a** as a yellow-green solid (135 mg). The filtrate was layered with pentane to precipitate 20 mg of additional solids, to give a total yield of 155 mg (71%). Complex **10a** is best recrystallized by slow diffusion of Et_2O into a saturated CH_2Cl_2 solution at −40 °C containing in a small amount of PMe_3, to avoid loss of PMe_3 to form **10b** (see below). IR (Nujol): 1630 (w, $\nu_{C{\equiv}C}$), 1426 (sh), 1413 (sh), 1296 (w), 1272 (w), 1161 (w), 954 (s), 851 (w), 668 (w). Anal. Calcd for $Mo_2SCl_4P_4C_{16}H_{42}$: C, 26.54; H, 5.85. Found: C, 26.21; H, 5.73.

$Mo_2(\mu\text{-}S)(\mu\text{-}CH_3C{\equiv}CCH_3)Cl_4(PMe_3)_3$ (10b). Complex **10b** was detected in high yield by NMR when a sample of **10a** was dissolved in 2 mL of toluene and stripped of volatiles 14 times, leaving a green residue.

$Mo_2(\mu\text{-}S)(\mu\text{-}CH_3C{\equiv}CCH_2CH_3)(PMe_3)_4Cl_4$ (11). Treatment of a suspension of 10 mg of **2** (1.5 × 10^{-2} mmol) in 0.5 mL of C_6D_6 with 0.13 mmol of 2-pentyne gas (9 equiv) gave a mixture of **11** and **2** by ^1H and $^{31}P\{^1H\}$ NMR, in a 1:2 ratio after 5 h and a 2:1 ratio after 2 weeks at ambient temperatures (which was unchanged after heating at 65 °C for 1 day).

Mo(*p*-TolC≡C-*p*-Tol)$Cl_2(PMe_3)_3$ (12). A solution of 200 mg of $MoCl_2(PMe_3)_4$ (0.42 mmol) and 96 mg of di-*p*-tolylacetylene (0.47 mmol; 1.1 equiv) in 8 mL of THF was heated at 80 °C for $^1/_2$ h. The volatiles were stripped under vacuum, the resulting solids were redissolved in 5 mL of toluene, and the solution was layered with 5 mL of Et_2O. Sitting overnight at −40 °C deposited green crystals of **12**, which were collected and washed with ether and pentane (190 mg). An additional 30 mg was obtained from further crystallization of the filtrate, to give a total yield of 220 mg (87%). ^1H NMR (THF-d_8): 7.10, 6.93 (both 4H, d, 8 Hz, $CH_3C_6H_4C{\equiv}CC_6H_4CH_3$), 2.31 (6H, s, $CH_3C_6H_4C{\equiv}CC_6H_4CH_3$), 1.41 (18H, t, 4 Hz, *trans*-$P(CH_3)_3$), 1.34 (9H, d, 8 Hz, *cis*-$P(CH_3)_3$). $^{31}P\{^1H\}$ NMR (THF-d_8): 6.1 (t, 16 Hz, *cis*-$P(CH_3)_3$), −1.24 (d, 16 Hz, *trans*-$P(CH_3)_3$). $^{13}C\{^1H\}$ NMR (THF-d_8): 225.3 (m, $CH_3C_6H_4C{\equiv}CC_6H_4CH_3$), 143.4, 136.5, 129.1, 126.5 (all s, $CH_3C_6H_4C{\equiv}CC_6H_4CH_3$), 23.3 (m, *cis*-$P(CH_3)_3$), 21.3 (m, $CH_3C_6H_4C{\equiv}CC_6H_4CH_3$), 18.5 (m, *trans*-$P(CH_3)_3$). IR (Nujol): 1620 (w, $\nu_{C{\equiv}C}$), 1505 (sh), 1492 (sh), 1418 (sh), 1367 (sh), 1299 (m), 1279 (m), 1155 (w), 1108 (w), 1035 (w), 1015 (w), 953 (s), 856 (w), 822 (w), 802 (w), 669 (w). Anal. Calcd for $MoCl_2P_3C_{25}H_{41}$: C, 49.93; H, 6.87. Found: C, 50.06, H, 6.87.

X-ray Crystallographic Structure Determinations of $Mo_2(\mu\text{-}S)(\mu\text{-}Cl)Cl_3(PMe_3)_4{\cdot}C_7H_8$ (2), $[Mo_2(\mu\text{-}S)(\mu\text{-}Cl)Cl_4(PMe_3)_4]NMe_4$ (5[NMe_4]), $Mo_2(\mu\text{-}S)(\mu\text{-}Cl)Cl_3(PMe_3)_4(CH_3CN)$ (6), and $Mo_2(\mu\text{-}S)(\mu\text{-}CH_3C{\equiv}CCH_3)Cl_4(PMe_3)_4$ (10a). Single crystals of **2**·C_7H_8 were grown by slow diffusion of petroleum ether into a saturated toluene solution of the complex at −12 °C over $1^1/_2$ weeks. Dark blue crystals of **5**[NMe_4] and brown crystals of **10a** were grown from NMR tube reactions of **2** + Me_4NCl in acetone-d_6 and **2** + 2-butyne in C_6D_6, respectively. Dark blue diamond-shaped plates of **6** were grown by layering a mixture of **2** in CH_3CN with petroleum ether and cooling to

(33) Erikson, T. K. G.; Bryan, J. C.; Mayer, J. M. *Organometallics* **1988**, *7*, 1930.

−40 °C. Crystals of **2** and **10a** were mounted in the drybox in sealed glass capillaries. Crystals of complexes **6** and **5**[NMe_4] were mounted in glass capillaries in air, and the capillaries were sealed under nitrogen. Data collection (24 °C) employed an Enraf-Nonius CAD4 diffractometer operating in the $\theta-2\theta$ scan mode with graphite-monochromated Mo $K\alpha$ radiation (λ = 0.71069), as previously described.[33] The structures of **2**, **5**[NMe_4], and **10a** were solved using the Siemens SHELX direct methods structure package. Space group determination for these complexes (*C2/c* for **2**; $P2_1/n$ for **5**[NMe_4]; *Pnma* for **10a**) was made on the basis of the fact that the structures did not solve as well in space groups with the same systematic absences. The structure of **6** was solved in $P\bar{1}$ directly from the Patterson map. All structures were refined with full-matrix least squares, and all non-hydrogen atoms, except the carbons of the toluene solvent molecule of **2**, were refined anisotropically. The positions of the hydrogen atoms were calculated (C−H = 0.95 Å) except the three hydrogens of the CH_3CN in **6**, which were located on a difference map and allowed to ride on the carbon atom during refinement. The assignments of the chloride and sulfide bridge were verified for **2** and **6** at an intermediate stage in the refinement by allowing the bridging ligands to be (1) both sulfides, (2) both chlorides, and (3) a chloride and a sulfide, but switched relative to their correct positions. Refinement of the structures for each of the three cases produced higher residuals and a poorer goodness of fit, shown as follows. The differences in the thermal parameters in the three cases were small and uninformative.

	complex **2**			
	case 1	case 2	case 3	final assignt
R_w	5.7	5.8	5.8	5.7
R	5.0	5.1	5.1	5.0
GOF	8.324	8.460	8.478	8.314
	complex **6**			
	case 1	case 2	case 3	final assignt
R_w	4.4	4.4	4.6	4.3
R	3.6	3.7	3.7	3.6
GOF	1.150	1.153	1.205	1.114

Acknowledgment. We thank Drs. David Barnhart and Susan Critchlow for assistance with the crystal structures, Dr. Tom Pratum for assistance with NMR experiments, Dr. David Clark for helpful discussions, and Prof. Rinaldo Poli for his comments on the manuscript. We are grateful to the National Science Foundation and the donors of the David M. Ritter Fellowship for generous financial support.

Supplementary Material Available: Tables of crystal data, anisotropic thermal parameters, hydrogen atom parameters, bond distances, ligand−ligand nonbonding distances, bond angles, torsion angles, and least-squares planes for **2**, **6**, **5**[NMe_4], and **10a** (33 pages). Ordering information is given on any current masthead page.

IC941153O